

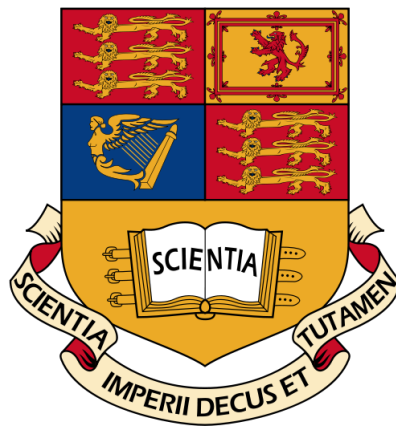
---

# Gauge-coupled curvaton preheating

---

Hans Wiermans

September 22, 2011



Submitted in partial fulfilment of the requirements for the degree of Master of Science of Imperial College London.

IMPERIAL COLLEGE LONDON  
DEPARTMENT OF PHYSICS

# Contents

<b>1</b>	<b>Introduction</b>	<b>3</b>
1.1	Historic introduction to inflation . . . . .	4
1.1.1	Magnetic monopole production in GUTs . . . . .	4
1.1.2	GUT phase transition and inflation . . . . .	5
1.1.3	The horizon problem . . . . .	6
1.1.4	The flatness problem . . . . .	8
1.2	Ending inflation . . . . .	9
1.2.1	Original idea . . . . .	9
1.2.2	Slow-roll inflation . . . . .	10
1.3	From GUT symmetry breaking to inflaton . . . . .	11
<b>2</b>	<b>Single field inflation</b>	<b>11</b>
2.1	Inflation from a single scalar field . . . . .	12
2.1.1	Homogenous part . . . . .	12
2.1.2	Slow-roll conditions . . . . .	13
2.2	Perturbations to the inflaton . . . . .	14
2.2.1	Perturbed field equation . . . . .	14
2.2.2	The inflaton power spectrum . . . . .	15
2.3	Curvature perturbation . . . . .	17
2.3.1	Separate universe approximation . . . . .	17
2.3.2	Curvature power spectrum . . . . .	18
2.3.3	Spectral index . . . . .	18
2.3.4	Non-Gaussian curvature perturbations . . . . .	20
<b>3</b>	<b>Curvaton model</b>	<b>20</b>
3.1	Basics of the curvaton model . . . . .	21
3.1.1	Curvaton field perturbation . . . . .	21
3.1.2	An evolving curvature perturbation . . . . .	22
3.2	Curvature perturbations in the curvaton model . . . . .	22
3.2.1	Oscillatory epoch . . . . .	22
3.2.2	The curvature perturbation . . . . .	23
3.2.3	Evaluating the non-Gaussianity . . . . .	25
3.3	The decay channel . . . . .	26
<b>4</b>	<b>Resonant curvaton decay</b>	<b>26</b>
4.1	Parametric decay into scalar field . . . . .	27
4.1.1	Evolution of the curvaton . . . . .	27
4.1.2	The $\chi$ field equation and resonance in a non-expanding universe . . . . .	28

4.1.3	Stochastic resonance in an expanding universe . . . . .	29
4.1.4	Adiabatic representation and particle density . . . . .	31
4.1.5	Back-reaction . . . . .	33
4.2	The curvature perturbation . . . . .	34
4.2.1	Separate universe approximation revisited . . . . .	34
4.2.2	Curvature perturbation without resonance . . . . .	35
4.2.3	Curvature perturbation from resonant decay . . . . .	36
4.3	Gauge coupled curvaton resonance . . . . .	38
4.3.1	Evolution of the curvaton . . . . .	38
4.3.2	The gauge field equation . . . . .	39
4.3.3	Stochastic resonance of the gauge field . . . . .	41
4.3.4	Back-reaction . . . . .	42
4.4	Curvature perturbation from gauge-field resonance . . . . .	46
<b>5</b>	<b>Discussion</b>	<b>47</b>
5.1	Comparison with scalar resonance . . . . .	47
5.2	Numerical simulations . . . . .	48

# 1 Introduction

This thesis discusses a method of generating curvature perturbations in the early universe using the curvaton model. This particular model assumes a light scalar field to be present in the very early stages of the universe, perturbations in which eventually lead to perturbations of the spacetime curvature. These curvature perturbations are the seeds for the structure we observe in the universe today, both in terms of (dark) matter distribution and in the cosmic microwave background, or CMB. Scalar fields in the early universe have been studied extensively since the discovery of inflation in the early 1980s [1]. Later, inflationary theories got a huge experimental boost because they could explain the existence of a near scale-invariant power spectrum of curvature perturbations as observed in the CMB.

Most inflationary theories predict this form of the curvature power spectrum, which has subsequently been confirmed by the COBE and WMAP experiments [2]. The new challenge is to exclude particular theories by comparing their prediction of non-Gaussianities in the curvature power spectrum with experimental results. Although the Gaussian part of the power spectrum has now been measured in great detail, upcoming measurements to be performed by the Planck satellite might be able to measure non-Gaussian parts to the curvature perturbation, as long as these are not too small [3].

In this thesis we discuss one particular model which could lead to large and observable non-Gaussianities in the curvature power spectrum. This is the model of curvaton preheating, in which the scalar curvaton field decays into another field during a period of parametric resonance. This resonance leads to a period of nonlinear dynamics, during which large non-Gaussianities may be generated. The name preheating stems from earlier models [4, 5, 6, 7] in which the inflaton decayed into another scalar field through a parametric resonance. In more recent articles [8, 9], the same approach has been applied to the curvaton, which has similar properties to the inflaton, but is subdominant in the energy density during inflation.

New in this thesis is the case in which the curvaton resonantly decays into a  $U(1)$  gauge field. This process shows many similarities with the scalar field resonance, but there are a few subtleties that arise when trying to apply the original methods of preheating to a gauge-scalar interaction.

The structure of this thesis is as follows. In the remainder of this section, we will present a general and historic introduction to inflation. This is intended to give less experienced readers some background information and to put the subsequently introduced models into an appropriate context. In section 2 we discuss how curvature perturbations are generated in the simplest single field inflationary models and show that this leads to a near scale-invariant power spectrum. In section 3 we introduce the curvaton model and discuss the canonical way in which this

model can generate curvature perturbations with higher levels of non-Gaussianity. In section 4 we discuss the curvaton preheating model. We discuss the parametric resonance and calculate the resulting curvature perturbation. Then we apply the same methods to a gauge-coupled curvaton model and we consider the curvature perturbation. Finally, in section 5 we discuss the differences between the scalar resonance and the new gauge-coupled. We also look ahead towards possible future numerical simulations, which are necessary to perform the full nonlinear calculation.

A note on conventions: throughout this thesis we will use the  $(-+++)$  signature for the Minkowski metric, we will work in natural units  $\hbar = c = G = k_B = 1$  and we will work with a standard FRW metric, which can be written as:

$$ds^2 = -dt^2 + a^2(t) \left[ \frac{dr^2}{1 - \kappa r^2} + r^2(d\theta^2 + \sin^2 \theta d\phi^2) \right], \quad (1.1)$$

where  $a(t)$  is the scale factor and  $\kappa$  the spatial curvature.

## 1.1 Historic introduction to inflation

In this section we will describe the basics of inflation: the discovery, the basic workings of the theory and the problems it solves in standard FRW cosmology. Although the main focus of this thesis is the curvaton model and the way in which curvature perturbations can be generated, it is important to note that this is a particular model of inflation. Therefore we included this section to give the non-experienced reader some background information on the theory of inflation.

### 1.1.1 Magnetic monopole production in GUTs

After the successes of electroweak unification, theoretical physicists in the 1970s started working on a theory that would combine the electroweak force with the strong force in a so-called “Grand Unified Theory”, or GUT for short. The earliest models were based on an  $SU(5)$  gauge theory, which would spontaneously break down into the  $SU(3) \times SU(2) \times U(1)$  standard model at an energy scale of  $\sim 10^{16}$  GeV (the so-called GUT-scale).

There is no way we can do experiments at this energy scale here on earth with current technology and most likely with any technology in the foreseeable future. There was however a time when GUT physics would have been valid. In the standard hot big bang model, there is a time in the very early universe when the energy scale is above the GUT-scale. However, as the universe expands, the energy density drops and when it reaches the GUT-scale a process of symmetry breaking occurs, which is similar to the  $SU(2) \times U(1) \rightarrow U(1)_{\text{em}}$  breaking in the Weinberg-Salam model.

One of the predictions of most GUTs is the existence of magnetic monopoles: particles with a fixed magnetic charge. These particles are obviously different from standard model particles, which do not have magnetic charge. As the energy of the universe drops below the GUT-scale, the interaction between monopoles and the other particles freezes out and the abundance of magnetic monopoles is fixed. To date, no magnetic monopoles have been found in nature, so their number density must be quite small, especially since GUT monopoles are believed to be very massive ( $10^{16}$  times heavier than the proton).

In the late 1970s people started doing research on the effects of magnetic monopoles on cosmology. It was found that the number density of monopoles is about equal to the number density of protons and neutrons [10]. Apart from the problem that monopoles had never been detected before this implied another, even bigger problem: the huge mass of the monopoles would have caused such a great gravitational force that the universe would have hardly expanded at all and could not be older than 1200 years, whereas we know that the universe is more than 10 billion years old. This over-abundance of magnetic monopoles in the theories became known as the “magnetic monopole problem”.

### 1.1.2 GUT phase transition and inflation

Just like with electroweak symmetry breaking, GUT symmetry breaking occurs because there is a potential for a scalar (or Higgs) field which has the full gauge symmetry at a local extremum, which is not the true vacuum. This local extremum is called the *false vacuum*. At early times the universe is in this false vacuum, which can have a much higher energy than the true vacuum. The energy density of the field in this false vacuum is constant. This means that, as the universe expands, the total energy increases which implies the scalar field has a negative pressure. The gravitational effect of this is similar to a cosmological constant, as long as in the equation of state:

$$p = w\rho, \tag{1.2}$$

the equation of state parameter  $w < -1/3$ . From the acceleration equation (second Friedmann equation):

$$\frac{\ddot{a}}{a} = -\frac{4\pi G}{3}\rho(1 + 3w), \tag{1.3}$$

we can see that in this case  $\ddot{a}/a > 0$ , which implies an accelerating scale factor. The solution for such an accelerating scale factor is the De Sitter solution, given by:

$$a(t) = C_1 e^{Ht} + C_2 e^{-Ht}, \tag{1.4}$$

where  $H = (-\frac{4\pi G}{3}\rho(1 + 3w))^{1/2}$  is the Hubble rate, which in this case is constant. Although the integration constants can be fixed by using the (first) Friedmann

equation, at times later than about one Hubble time  $H^{-1}$  all solutions will practically look like exponential growth:  $a(t) \sim e^{Ht}$ .

In only  $10^{-35}$ s, the universe would have undergone 100 e-folds, which would have increased its size by a factor  $10^{30}$ . Clearly, such a scenario would drastically lower the number density of magnetic monopoles. The first person to discover this gravitational effect of the false vacuum state of the GUT Higgs field was Alan Guth. He is subsequently considered the one who discovered inflation, which he first described in [1]. As we can see from the title of his classic paper, inflation can solve several other problems which Guth considered clearly more important than the monopole problem.

### 1.1.3 The horizon problem

The horizon problem has to do with the amount of homogeneity we see across the entire sky, for instance when looking at the cosmic microwave background. Although experiments like COBE and WMAP have mapped the small anisotropies in the CMB, which provide the experimental basis for the work done in this thesis, overall the CMB is incredibly smooth and isotropic. Since any information can only travel as fast as the speed of light, the only reason why the universe would look exactly the same in all directions, is because all those regions were in causal contact when the universe was much smaller.

However, if we calculate the *comoving horizon distance*, which is the maximum distance any particle can have travelled from an initial time ( $t = 0$ ) to a particular time  $t_0$ , rescaled by the expansion of the universe, (this is equivalent to conformal time, multiplied by the speed of light). We can write this as:

$$\eta(t_0) = \int_0^{t_0} \frac{dt}{a(t)}. \quad (1.5)$$

If we compare the comoving horizon distance at last scattering, when the CMB was created, with its current value, we find the ratio:

$$\frac{\eta(t_\star)}{\eta(t_0)} \approx 10^{-2}, \quad (1.6)$$

where  $t_\star$  is time of last scattering and  $t_0$  is today. Cubing this, we can see that the current observable universe consists of some  $10^6$  different regions that were causally disconnected when the CMB was created, yet it looks identical in every direction. The problem becomes worse when we compare the horizon distance today with the horizon distance at the Planck time. Then we have:

$$\frac{\eta(t_P)}{\eta(t_0)} \approx 10^{-26}, \quad (1.7)$$

which means the current observable universe consists of  $10^{78}$  regions that were causally disconnected at the Planck time.

To see how a period of inflation can help solve this, problem, let us change variables and rewrite equation (1.5) as:

$$\eta(a_0) = \int_0^{a_0} d \ln a \frac{1}{aH}, \quad (1.8)$$

where  $H = \dot{a}/a$  is the Hubble parameter, so  $1/aH$  is the comoving Hubble radius (or time). This quantity gives us the maximum distance between two points that are in causal contact at any particular time. If the comoving Hubble radius was much bigger in the past than it is now and then decreased in size, regions that were once causally connected would have fallen out of causal contact. The only way for the comoving Hubble radius to decrease is to have  $\ddot{a} > 0$ , i.e. a period in which the expansion of the universe is accelerating: inflation.

We can calculate the number of e-foldings inflation must have lasted in order to solve the horizon problem. To do this, we look at the current size of the comoving Hubble radius  $1/a_0 H_0$  and argue that, before inflation, this must have been as least this large. Then during inflation the comoving Hubble radius decreased rapidly, only to slowly increase from the end of inflation until today. To see how much the comoving Hubble radius must have decreased during inflation, we first calculate how much it has grown after. For this, we assume the universe to be radiation dominated for the rest of its history. This is because, for a radiation dominated universe with  $a \sim t^{1/2}$  we have  $1/aH \sim a$ , while for a matter dominated universe with  $a \sim t^{2/3}$ , the comoving Hubble radius only grows as  $1/aH \sim a^{1/2}$ .

Using this scaling law, we can calculate the ratio of the current comoving Hubble radius with the one just after the end of inflation, as:

$$\frac{1}{a_0 H_0} = \frac{a_0}{a_f} \frac{1}{a_f H_f} = \frac{T_{\text{GUT}}}{T_0} \frac{1}{a_f H_f}, \quad (1.9)$$

where we made use of the fact that during radiation domination  $a \sim T$  and we assumed inflation happens at temperatures around the GUT scale, with  $T_{\text{GUT}} \sim 10^{16}$  GeV. Under these assumptions and using the current temperature of the CMB (2.7K), it is easy to see that:

$$\frac{1}{a_0 H_0} = 10^{29} \frac{1}{a_f H_f}, \quad (1.10)$$

i.e. for inflation to solve the horizon problem, the comoving Hubble radius had to decrease by at least 29 orders of magnitude during inflation. Since  $H$  is nearly constant during inflation, this would mean the scale factor had to increase by 29 orders of magnitude, i.e.:

$$\frac{a_f}{a_i} = e^{H(t_f - t_i)} \equiv e^N = 10^{29}, \quad (1.11)$$



with  $a_i$  and  $a_f$  the scale factors directly before and after inflation, respectively. This implies inflation solves the horizon problem if it lasts for a minimum of  $N = \ln(10^{29}) = 67$  e-foldings.

#### 1.1.4 The flatness problem

From various measurements we can deduce that the universe is nearly spatially flat, which means  $\kappa = 0$  in the first Friedmann equation:

$$H^2 = \frac{\rho}{3m_P^2} - \frac{\kappa}{a^2}. \quad (1.12)$$

This equation can be rewritten in terms of the critical energy density  $\Omega = \rho/\rho_{crit}$ , where  $\rho_{crit} = 3m_P^2 H^2$  as:

$$\Omega_\kappa \equiv \Omega - 1 = \frac{\kappa}{a^2 H^2} \quad (1.13)$$

and  $\Omega$  contains contributions of matter and radiation (and possibly a cosmological constant). Now the problem lies in the fact that  $\Omega$  is *approximately* 1. Since in general the expansion rate of the universe  $\dot{a}$  has been decreasing, this means that  $\Omega - 1$  has been getting progressively larger.

During the period of matter domination, when  $a \sim t^{2/3}$ , this means  $\Omega_\kappa \sim t^{2/3}$ , while during radiation domination, when  $a \sim t^{1/2}$ , we have  $\Omega_\kappa \sim t$ . Combined data [2] shows that currently  $\Omega_\kappa(t_0) < 0.01$ . If we assume the initial conditions were set at the Planck time ( $10^{-43}$ s), use the current age of the universe ( $\sim 10^{17}$ s) and assume matter-radiation equality happened at  $\sim 10^{11}$ s, then we can calculate how small  $\Omega_\kappa$  must have been at initially:

$$\Omega_\kappa(t_P) < 10^{-61}, \quad (1.14)$$

i.e. to explain the current flatness of the universe, one must fine-tune the initial flatness of the universe to an extreme amount. Of course, the problem vanishes if one assumes the universe to be perfectly flat ( $\kappa = 0$ ), since in this case  $\kappa$  will remain zero forever in the past and future. Although this is in agreement with observations, there is no reason why  $\kappa$  should be exactly zero. In fact, assuming this might be as arbitrary as fine-tuning it to one part in  $10^{61}$ .

Inflation provides a much more elegant solution to this problem, without having to make any of these assumptions. Again, the solution relies on the fact that  $\ddot{a} > 0$  during inflation. During most of the lifetime of the universe,  $\dot{a}$  has been decreasing and the deviation from flatness has been growing. However, if we had a period of exponential growth in the early universe, then this would have caused  $\dot{a}$  to grow enormously, which would have destroyed any significant deviation from flatness that was present initially (at  $t_P$ ).

## 1.2 Ending inflation

Now that we have looked at the possible solutions that inflation can provide for several large cosmological problems, we now turn our attention to the problem that plagued all early inflationary models: how does inflation end?

### 1.2.1 Original idea

In Guth's original paper [1], the universe starts out in the unbroken symmetry phase (false vacuum). During inflation, bubbles of the broken symmetry phase form. This happens through a tunneling process, which is shown in figure 1: in every region in space there is a probability the field can tunnel through the potential barrier and end up in the true vacuum state.

Within these bubbles, the energy released by the transition would have gone into the bubble walls. The original idea was that as these bubbles grow, they collide and when they do the energy stored in the walls would thermalise the universe, leading to the starting point of standard big bang nucleosynthesis (BBN). However, while the bubbles of the new phase are forming and growing, the whole universe is expanding exponentially, which could mean the bubbles would never collide and thermalise the universe. Furthermore, a large part of the universe would remain in the symmetric phase, which means inflation would never stop. This became known as the *graceful exit problem*. This was already recognised in the original paper [1] and confirmed just a few months later [11].

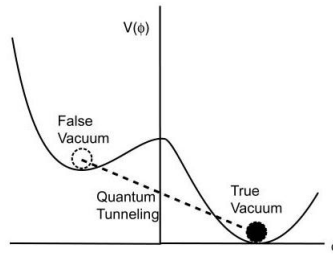


Figure 1: Original potential for the inflaton field. The field is trapped in a false (metastable) vacuum, with a probability of tunneling to the true vacuum. In the regions where this happens, inflation suddenly ends and a bubble of the true vacuum (broken symmetry) phase forms. Ref: [12].

### 1.2.2 Slow-roll inflation

Only a few months later, several papers appeared [13, 14] which solved this graceful exit problem by introducing a different mechanism of symmetry breaking, called the Coleman-Weinberg (CW) mechanism. Here, the shape of the potential dramatically depends on the temperature of the universe. This is shown pictorially in figure 2. At early times, the symmetric phase is the true (stable) vacuum. However, as the temperature decreases, the slope of the potential starts to decrease and a second local minimum forms at some field value where the full gauge symmetry is broken. As the temperature of the universe drops below the critical GUT-scale  $T_c = T_{\text{GUT}} \sim 10^{16}\text{GeV}$ , the energy of the broken symmetry phase drops below the symmetric phase, which becomes metastable.

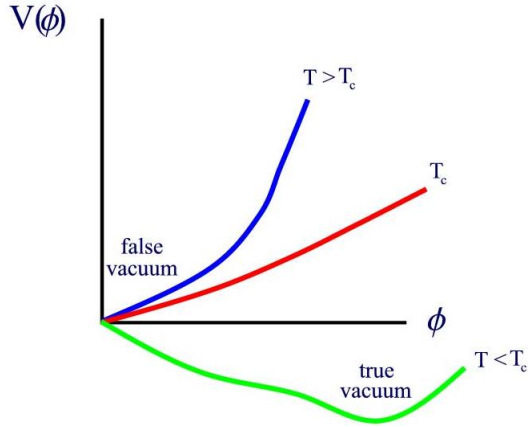


Figure 2: The Coleman-Weinberg mechanism: the shape of the scalar field potential changes with the background temperature of the universe. As  $T < T_c$ , the gauge-symmetric phase  $\phi = 0$  is no longer a local minimum and the field starts to slowly roll down the potential until it settles into some broken-symmetry vacuum phase. Ref: [12].

However, unlike the original scenario, this time the potential is very flat from the symmetric phase to the broken symmetry phase. As the temperature drops below  $T_{\text{GUT}}$ , the field starts to roll slowly down the flat potential towards the true vacuum. The regions (bubbles) in which this transition occurs therefore undergo a much longer period of inflation than in the original scenario, which causes them to grow by many e-foldings. As a result, in such models our entire observable universe is contained in just a small fraction of one such bubble. This immediately solves the three cosmological problems discussed earlier. Because of the enormous expansion, the number density of monopoles is diluted down to a tiny amount, so

we wouldn't expect to see any monopoles at all. The expansion also takes care of the flatness problem. Because the whole observable universe lies within one bubble, this would explain the large homogeneity of our universe and it would also explain why we don't observe any domain walls or other topological defects.

### 1.3 From GUT symmetry breaking to inflaton

The previous section gave a historic account of the theory of inflation. As we have seen, inflation was discovered in the context of magnetic monopole production in GUT phase transitions, where it was found to solve the monopole problem. Then it was realised this could also solve the horizon and flatness problems. While the promise of solving these problems sparked the initial interest in inflationary models, these are “only” naturalness problems. Nowadays there is much more solid, experimental evidence to support a period of inflation. Measurements of the CMB temperature fluctuations performed by WMAP [2], reveal a nearly scale-invariant power spectrum of density perturbations in the early universe. This form of the power spectrum is exactly the one predicted by slow-roll inflation. This experimentally rules out the oldest models of inflation with a false vacuum, since these models do not generate the required density perturbations.

In early inflationary models, the scalar field responsible for the exponential expansion was a Higgs field from Grand Unified Theories. However, the GUTs that were considered, including the simple and elegant Georgi-Glashow model [15] predicted an unstable proton with a lifetime that has since been disproved by experiments. While inflation became ever more accepted as a real period in the history of the universe, there is to date no certainty that GUTs actually exist. This led people to consider models where the scalar field that drives inflation is not related to any GUT. This field is called the inflaton. In section 2 we will consider this field in more detail and we show how it leads to inflation and the scale-invariant density perturbations.

Many more advanced models of inflation have since been proposed, including models that contain multiple fields. One such multi-field model, called the curvaton model, is the focus of this paper and will be introduced in section 3.

## 2 Single field inflation

In this section we review the simplest model of slow-roll inflation: the single field model. This model consists of a single scalar field (the inflaton)  $\phi$ , which causes exponential expansion of the universe while slowly rolling down a potential. As it nears the end of the potential, it starts to oscillate and transfer its energy. We will

show that this oscillation leads to a nearly scale-invariant spectrum of curvature perturbations.

## 2.1 Inflation from a single scalar field

The inflaton is a scalar field  $\phi$  which is assumed to be nearly homogeneous. Therefore we can write it as:

$$\phi(\mathbf{x}, t) = \phi(t) + \delta\phi(\mathbf{x}, t), \quad (2.1)$$

where  $\delta\phi \ll \phi$  is a small perturbation. To derive the equations of motion (Friedmann equations) for this scalar field, we have to know its energy density and pressure. These can be obtained from the stress energy tensor, which for a scalar field is given by:

$$T_{\beta}^{\alpha} = g^{\alpha\nu} \frac{\partial\phi}{\partial x^{\nu}} \frac{\partial\phi}{\partial x^{\beta}} - g_{\beta}^{\alpha} \left[ \frac{1}{2} g^{\mu\nu} \frac{\partial\phi}{\partial x^{\mu}} \frac{\partial\phi}{\partial x^{\nu}} + V(\phi) \right], \quad (2.2)$$

where we can use the Minkowski metric  $g_{\mu\nu} = \eta_{\mu\nu}$ , as long as gravity is weak.

### 2.1.1 Homogenous part

Although the field perturbations  $\delta\phi$  are essential for understanding the curvature perturbations, if we want to see how a period of inflation arises, we just need to look at the homogeneous part  $\phi(t)$ . In that case the spatial derivatives vanish and we are left with:

$$T_{\beta}^{\alpha} = -\eta_0^{\alpha} \eta_{\beta}^0 \dot{\phi}^2 + \eta_{\beta}^{\alpha} \left[ \frac{1}{2} \dot{\phi}^2 - V(\phi) \right], \quad (2.3)$$

where the dot represents the derivative w.r.t. time. From this expression we can distill the two quantities of interest:

$$\begin{aligned} \rho = -T_0^0 &= \frac{1}{2} \dot{\phi}^2 + V(\phi) \\ P = T_i^i &= \frac{1}{2} \dot{\phi}^2 - V(\phi), \end{aligned} \quad (2.4)$$

from which we see that the field generates a negative pressure as long as the potential energy is greater than the kinetic term. More precisely, if we look at the acceleration equation (1.3), we see that the inflaton generates an accelerating scale factor as long as  $V > \dot{\phi}^2$ . The Friedmann equations now become:

$$\begin{aligned} \left( \frac{\dot{a}}{a} \right)^2 &= \frac{1}{3m_P^2} \left[ \frac{\dot{\phi}^2}{2} + V \right] \\ \frac{\ddot{a}}{a} &= -\frac{1}{3m_P^2} \left[ \dot{\phi}^2 - V \right]. \end{aligned} \quad (2.5)$$

Differentiating the first Friedmann equation and plugging both of (2.5) into the LHS gives us the equation of motion for  $\phi$ :

$$\ddot{\phi} + 3H\dot{\phi} + V' = 0, \quad (2.6)$$

where  $V' = dV/d\phi$ .

### 2.1.2 Slow-roll conditions

We discussed the concept of slow-roll inflation in section 1.2.2 and we will now quantify what is meant by this. Basically it means we ignore the  $\dot{\phi}$  term in the Friedmann equation and ignore the  $\ddot{\phi}$  term in the field equation (2.6), so we have:

$$3H\dot{\phi} = -V'. \quad (2.7)$$

This approximation will only hold under two conditions:

$$\epsilon(\phi) \ll 1 \quad \text{and} \quad |\eta(\phi)| \ll 1, \quad (2.8)$$

where

$$\begin{aligned} \epsilon(\phi) &= \frac{m_P^2}{2} \left( \frac{V'}{V} \right)^2 \\ \eta(\phi) &= m_P^2 \frac{V''}{V} \end{aligned} \quad (2.9)$$

are the so-called slow-roll parameters.

To see how the slow-roll approximation leads to a period of inflation, we rewrite the condition of inflation as:

$$\frac{\ddot{a}}{a} = \dot{H} + H^2 > 0. \quad (2.10)$$

This is obviously satisfied if  $\dot{H} > 0$ , but this violates the dominant energy condition  $-\rho < P < \rho$  which, as we can see from (2.4), is not possible for a scalar field. The required condition is therefore  $-\dot{H}/H^2 < 1$  which, in the slow-roll approximation, can be written as:

$$-\frac{\dot{H}}{H^2} \simeq \frac{m_P^2}{2} \left( \frac{V'}{V} \right)^2 = \epsilon < 1. \quad (2.11)$$

Since the slow-roll condition is  $\epsilon \ll 1$ , we can see that when the slow-roll conditions hold,  $\ddot{a} > 0$  and inflation is guaranteed.

## 2.2 Perturbations to the inflaton

Although we can understand inflation by just looking at the homogenous part of  $\phi$ , the perturbations to this background are much more important. Perturbations to the inflaton field lead to primordial curvature perturbations, which are responsible for the structure that is visible in the present-day universe and in the CMB. In this section we show that a slow-roll single field model of inflation leads to a nearly Harrison-Zeldovich scale-invariant power spectrum of curvature perturbations.

### 2.2.1 Perturbed field equation

In section 2.1.1 we derived (2.6) assuming  $\phi$  was a homogenous field. If we now want to consider a space-dependent field, we can obtain the inflaton field equation more easily by using the Euler-Lagrange equations. From the Lagrangian:

$$\mathcal{L} = -\frac{1}{2}(\partial_\mu\phi)(\partial^\mu\phi) - V(\phi) \quad (2.12)$$

we obtain the free scalar field equation of motion:

$$-\square\phi + V'(\phi) = 0, \quad (2.13)$$

where the d'Alembertian operator  $\square$  in curved spacetime is given by [16]:

$$\square\phi = \frac{1}{\sqrt{-g}}\partial_\mu(\sqrt{-g}g^{\mu\nu}\partial_\nu\phi). \quad (2.14)$$

Using this expression with the FRW metric (1.1), where  $\sqrt{-g} = \sqrt{-\det(g_{\mu\nu})} = a^{-3}$  the we obtain:

$$\begin{aligned} -\square\phi &= \frac{1}{a^3}(3a^2\dot{a}\dot{\phi} + a^3\ddot{\phi}) - \frac{1}{a^3}\partial_i(a\partial_i\phi) \\ &= \ddot{\phi} + 3H\dot{\phi} - (a^{-1}\partial_i)^2\phi, \end{aligned} \quad (2.15)$$

Plugging this into (2.13) leads to the space-dependent version of (2.6):

$$\ddot{\phi} + 3H\dot{\phi} - \nabla^2\phi + V' = 0, \quad (2.16)$$

where  $\nabla$  is the del-operator in comoving coordinates  $\nabla_i = a^{-1}\partial_i$  and  $\phi(\mathbf{x}, t)$  is the full inflaton field. To obtain an equation of motion for the perturbations we perturb (2.16), which up to first order gives us:

$$\delta\ddot{\phi} + 3H\delta\dot{\phi} - \nabla^2\delta\phi + V''\delta\phi = 0. \quad (2.17)$$

It is useful in cosmological perturbation theory to work with the Fourier transform of  $\delta\phi$ , because this allows us to compare the wavelength of a perturbation

mode with the size of the comoving Hubble radius (or horizon). The Fourier transform of (2.17) is given by:

$$\delta\ddot{\phi}_{\mathbf{k}} + 3H\delta\dot{\phi}_{\mathbf{k}} - \left(\frac{k}{a}\right)^2 \delta\phi_{\mathbf{k}} + \frac{1}{2}V''\delta\phi_{\mathbf{k}} = 0. \quad (2.18)$$

As we will henceforth only work with the Fourier modes of the perturbation, we will drop the subscript  $\mathbf{k}$  from now on.

A simple potential which is often used is a quadratic one,  $V(\phi) = \frac{1}{2}m^2\phi^2$ , where  $m$  can be interpreted as the inflaton's mass. Using this potential, we have  $V'' = m^2$  and the slow-roll condition can be written as:

$$m^2 \ll \frac{V}{m_P^2} \simeq H^2, \quad (2.19)$$

which implies we can ignore the last term in (2.18). This means that, during inflation, the inflaton can be considered a massless field and the equation of motion becomes:

$$\delta\ddot{\phi} + 3H\delta\dot{\phi} - \left(\frac{k}{a}\right)^2 \delta\phi = 0. \quad (2.20)$$

Modes in the sub-horizon limit ( $k \gg aH$ ), behave as a harmonic oscillator:

$$\delta\ddot{\phi} + \left(\frac{k}{a}\right)^2 \delta\phi = 0. \quad (2.21)$$

As a mode exits the horizon, the damping term becomes important and the mode “freezes out” to a constant value.

We should note at this point that we made a linear approximation here, which in the language of perturbation theory means we are treating  $\delta\phi$  as field free of interactions. In particular, there is no self-interaction between the different Fourier modes, which could lead to non-Gaussianity.

### 2.2.2 The inflaton power spectrum

A general solution to (2.20) is a damped oscillator. In the regime a few  $H^{-1}$  before and after horizon exit, which is the period we're interested in, we can take  $H$  to be constant. A solution is then given by:

$$\delta\phi(t) = L^{-3/2} \frac{H}{(2k^3)^{1/2}} \left[ i + \frac{k}{aH} \right] \exp\left(\frac{ik}{aH}\right), \quad (2.22)$$

where  $L$  is the box size that comes in with the Fourier transform. In this solution, the exponential takes care of the oscillatory behaviour, while the second term



in brackets takes care of the damping. The precise amplitude is obtained by matching the solution to the initial conditions set at the Planck time. Neglecting the exponential, we have that as  $t \rightarrow -\infty$ ,  $aH \rightarrow 0$  and the solution approaches:

$$\delta\phi \rightarrow \frac{1}{(2ka^2V)^{1/2}}, \quad (2.23)$$

where  $V = L^3$ . This is in terms of comoving coordinates. It can be written in terms of physical coordinates  $k_{phys} = k/a$  and  $V_{phys} = a^3V$  as:

$$\delta\phi \rightarrow \frac{1}{\sqrt{V_{phys}^{1/2}}} \frac{1}{\sqrt{2k_{phys}}}. \quad (2.24)$$

If we assume quantum field theory to still be valid at this scale (which is a non-trivial assumption) then, as we are deep within the horizon, we can ignore the curvature of spacetime. Hence we can use the equal time commutation relation from QFT in Minkowski spacetime to give us the initial conditions for the field perturbation:

$$\langle |\delta\phi|^2 \rangle = \frac{1}{V} \frac{1}{2\omega_{\mathbf{k}}}. \quad (2.25)$$

Since in Minkowski space  $V = V_{phys}$  and in the ultra-relativistic limit  $\omega_{\mathbf{k}} = k$ , our solution in the  $t \rightarrow -\infty$  limit (2.24) limit matches up with the initial quantum fluctuation at the Planck time.

Since all the time dependence of (2.22) is in the scale factor, it is easy to check that:

$$\begin{aligned} \dot{\delta\phi} &= -L^{-3/2} \frac{H}{(2k^3)^{1/2}} \left[ \frac{ik^2}{a^2 H} \right] \exp\left(\frac{ik}{aH}\right) \\ \delta\dot{\phi} &= L^{-3/2} \frac{H}{(2k^3)^{1/2}} \left[ \frac{2ik^2}{a^2} - \frac{k^3}{a^3 H} \right] \exp\left(\frac{ik}{aH}\right). \end{aligned} \quad (2.26)$$

Plugging these into (2.20) shows (2.22) is indeed a solution. We have taken a slight shortcut here: we have solved a classical equation of motion for  $\delta\phi$ , while this is really a quantum field. In the Heisenberg picture of quantum mechanics, each Fourier mode of  $\delta\phi$  is a time-dependent operator, which can be written in terms of creation and annihilation operators. The time dependence is carried by the coefficients of those ladder operators. However, at the linear level, the time evolution of these coefficients is equal to the classical equation of motion, so we can treat the field classically.

We would like to obtain the power spectrum at a time ( $t = t_*$ ), a few  $H^{-1}$  after horizon exit when the modes have frozen out and the spectrum is fixed. The

power spectrum follows from the expectation value of  $\delta\phi$  and is given by:

$$\mathcal{P}_\phi(k, t) = \frac{L^3 k^3}{2\pi^2} \langle |\delta\phi(t)|^2 \rangle, \quad (2.27)$$

where again  $L$  is due to the Fourier transform and will drop out of the final answer. Since we treat the field classically, there is only one value for  $|\delta\phi|^2$ . At the time of interest  $t_*$ , a few Hubble times have already passed since horizon exit and  $k/aH \ll 1$ , so the modulus squared of  $\delta\phi$  is given by:

$$|\delta\phi(t)|^2 = \frac{H^2}{2L^3 k^3}, \quad (2.28)$$

plugging this into (2.27), this allows us to write down the power spectrum at  $t = t_*$ :

$$\mathcal{P}_\phi(k, t_*) = \left( \frac{H(t_*)}{2\pi} \right)^2 \simeq \left( \frac{H}{2\pi} \right)^2 \Big|_{k=aH}. \quad (2.29)$$

This last approximation is for definiteness. Since  $t_*$  is not a well-defined time and we assumed  $H$  to be nearly constant anyway, we might as well evaluate the power spectrum at the moment of horizon exit. As we can see, this power spectrum does not depend on  $k$ : it is scale-invariant. This scale invariance relies on a few approximations and we will see that in general the power spectrum will be slightly deviating from scale invariance. More on this in section 2.3.2.

## 2.3 Curvature perturbation

In the previous section, we found the power spectrum for the field  $\phi$ . Now we need to translate this into a curvature power spectrum. This primordial curvature power spectrum will then set the initial conditions for the evolution of structure in the universe. To derive a relation between field and curvature perturbations, we make use of the *separate universe approximation*.

### 2.3.1 Separate universe approximation

The separate universe approximation [17] relies on the fact that points in space separated by more than a Hubble radius will be out of causal contact and thus evolve independently. It is therefore possible to treat each Hubble volume as a separate FRW universe, as long as each region is roughly homogeneous and isotropic, so each “universe” has a homogeneous scale factor and energy density.

Within each “universe”, the curvature perturbation is given by the logarithm of the scale factor, evaluated at a constant energy density slicing:

$$\zeta = \delta \ln a \Big|_{\rho=\rho_{\text{end}}}, \quad (2.30)$$

where  $\delta$  denotes difference from the average value and  $\rho_{\text{end}}$  is an energy density at time  $t_{\text{end}}$  well after inflation has ended, when the curvature perturbation has frozen out. It is important to note that this is generally not the same time as  $t_*$ , which is when the field perturbation has frozen out. Although the two are equal in this simple single field model, in more complicated models including the curvaton model, the curvature perturbations still evolve after the fields have frozen out.

From observations of the CMB we know that the curvature spectrum is very Gaussian. Since the curvature perturbation depends on the Gaussian field perturbation  $\delta\phi$ , it therefore makes sense to approximate (2.30) by a Taylor series in  $\delta\phi$ . The curvature perturbation will then be Gaussian to leading order, with higher order terms giving non-Gaussian corrections:

$$\zeta = (\ln a)'|_{\rho} \delta\phi_* + \frac{1}{2}(\ln a)''|_{\rho} \delta\phi_*^2 + \mathcal{O}(\delta\phi_*^3) \quad (2.31)$$

In a single field model we assume the perturbation  $\delta\phi_*$  to be small compared to the average value of  $\phi$ , so the quadratic and higher order terms can be neglected. Using this linear approximation and the scale factor during inflation  $a = \exp(Ht)$ , the curvature perturbation becomes:

$$\zeta = (Ht)' \delta\phi_* = \frac{d(Ht)}{dt} \frac{dt}{d\phi} \delta\phi_* = \frac{H}{\dot{\phi}} \delta\phi_*. \quad (2.32)$$

### 2.3.2 Curvature power spectrum

Just like we did for the field perturbation, we can now write down the power spectrum for the curvature perturbations:

$$\mathcal{P}_{\zeta} = \frac{L^3 k^3}{2\pi^2} \langle |\zeta|^2 \rangle = \frac{L^3 k^3}{2\pi^2} \left( \frac{H}{\dot{\phi}} \right)^2 \langle |\delta\phi|^2 \rangle = \left( \frac{H}{\dot{\phi}} \right)^2 \left( \frac{H}{2\pi} \right)^2. \quad (2.33)$$

Because the field power spectrum (2.29) is scale-invariant, so is the curvature power spectrum. This scale-invariant spectrum relies on a few approximations though. If we look beyond these approximations, we will find slight deviations from scale-invariance. One of our assumptions was that  $H$  would be constant during inflation, but in reality it is slightly changing in time. This effects the solution for  $\delta\phi$  and thus the power spectrum.

### 2.3.3 Spectral index

The deviation from scale-invariance is captured by the *spectral index*  $n_s$ , which is defined as:

$$n_s(k) - 1 \equiv \frac{d \ln \mathcal{P}_{\zeta}}{d \ln k}, \quad (2.34)$$

which for a range of constant  $n_s$  essentially means:

$$\mathcal{P}_\zeta \propto k^{n_s-1}, \quad (2.35)$$

from which we see that the scale-invariant spectrum corresponds to  $n_s = 1$ . Data shows that the power spectrum observed in the CMB is close to scale invariant, but excludes the exact scale invariant case  $n_s = 1$  with great certainty [2]. This deviation from scale-invariance could very well be attributed to fact that the aforementioned approximations do not fully hold.

Because we know the rough form of the power spectrum (2.33) and it is evaluated at horizon exit  $k = aH$ , it is possible to evaluate the spectral index and express it in terms of the slow-roll parameters. We start by rewriting the power spectrum in terms of the slow-roll parameters. Using (2.7) and the critical energy density  $H^2 = V/3m_P^2$ , we can write:

$$\mathcal{P}_\zeta = \left(\frac{V}{m_P^2}\right)^2 \left(\frac{V}{12\pi^2 m_P^2}\right) = \frac{1}{24\pi^2 m_P^4} \frac{V}{\epsilon}. \quad (2.36)$$

Next, we evaluate the differential  $d \ln k$ . We have (at horizon exit):

$$\ln k = \ln a + \ln H. \quad (2.37)$$

Because during slow roll,  $H$  is nearly constant and most of the time dependence is in the scale factor, we have:

$$\frac{d \ln k}{dt} \approx \frac{d \ln a}{dt} = H. \quad (2.38)$$

Now we can switch variables from  $dt$  to  $d\phi$ . Again using the slow-roll approximation (2.7) and the critical density, we obtain:

$$\frac{d}{d \ln k} = -m_P^2 \left(\frac{V'}{V}\right) \frac{d}{d\phi}. \quad (2.39)$$

Using this, we find:

$$\frac{d \ln \mathcal{P}_\zeta}{d \ln k} = \frac{1}{V} \frac{dV}{d \ln k} + \frac{1}{\epsilon} \frac{d\epsilon}{d \ln k}, \quad (2.40)$$

and using

$$\frac{dV}{d \ln k} = -2\epsilon V \quad \text{and} \quad \frac{d\epsilon}{d \ln k} = -2\epsilon\eta + 4\epsilon^2, \quad (2.41)$$

this gives us:

$$n_s - 1 = 2\eta - 6\epsilon. \quad (2.42)$$

This immediately shows that, under slow-roll conditions (2.8), the spectral index is very close to scale-invariant. In the derivation of (2.42) we have still assumed  $H$  to be constant, or at least  $\dot{H} \ll \dot{a}$ . Relaxing this condition will generally give a larger deviation from scale-invariance.

### 2.3.4 Non-Gaussian curvature perturbations

In the single-field model, the final curvature perturbation (2.32) is Gaussian. This follows from the initial Planck-era vacuum fluctuation, which we assumed to be given by the standard flat spacetime ETCR (2.25) and which is a Gaussian quantity. The reason why this initial Gaussian fluctuation remains Gaussian until a much later era has to do with the linear approximations we made in deriving the equations of motion for the perturbation. A Gaussian distribution which evolves linearly will remain Gaussian. However, the linearity of equations (2.20) and (2.32) is due to first order Taylor approximations. If we include higher orders in those approximations, this will give us a non-Gaussian component of the curvature perturbation.

If we include higher order terms in the field equation (2.20), we will end up with a non-Gaussian field perturbation, but this would mean the field equation is no longer easy to solve analytically. Instead, we assume the linear approximation holds for the field equation and we include higher orders in (2.31). This would modify the dependence of  $\zeta$  on the field perturbation  $\delta\phi$  by adding a quadratic term to (2.32). Up to second order we write:

$$\zeta = \zeta_g + \frac{3}{5} f_{\text{NL}}(\zeta_g)^2, \quad (2.43)$$

where  $\zeta_g$  is the Gaussian curvature perturbation (2.32) obtained in the first order approximation. The factor  $3/5$  is there just by convention and  $f_{\text{NL}}$  is the *nonlinearity parameter*, which measures the size of the nonlinear and hence the non-Gaussian part of the curvature perturbation. Since the Gaussian part of the perturbation is  $(\ln a)' \delta\phi_*$  and the total perturbation is given by (2.31), the nonlinearity parameter is given to by:

$$f_{\text{NL}} = \frac{5}{6} \frac{(\ln a)''}{(\ln a)'^2} \Big|_{\rho}. \quad (2.44)$$

## 3 Curvaton model

In the previous section we described a simple model of slow-roll inflation, where there is a single field  $\phi$  which is responsible for generating the era of inflation as well as the primordial curvature perturbations. The beauty of this model of course lies in its simplicity, while it also predicts the nearly scale-invariant curvature spectrum as observed in the CMB. However, as discussed in section 2.3.4, it is hard for such a model to generate significant non-Gaussianity in the curvature spectrum. However, other models might lead to greater non-Gaussianity in the curvature spectrum which, if present, could be measured by future experiments such as Planck [3].

In this section we will introduce the model which is the focus of this thesis: the curvaton model [18, 19].

### 3.1 Basics of the curvaton model

The basic idea of the curvaton model is to have two light scalar fields during inflation instead of one. We still have the inflaton  $\phi$ , which drives inflation, just as described in section 2.1. However, in addition there is another scalar field  $\sigma$ , called the curvaton. The idea is that the inflaton just takes care of inflation, while the curvaton is the dominant force in generating the curvature perturbation. In the simplest case then, we will have a Lagrangian:

$$\mathcal{L} = \mathcal{L}_\phi + \frac{1}{2}\dot{\sigma}^2 - \frac{1}{2}(\nabla\sigma)^2 - \frac{1}{2}m^2\sigma^2, \quad (3.1)$$

where  $\mathcal{L}_\phi$  is the Lagrangian for the inflaton field and we assume a quadratic form for the curvaton potential  $V(\sigma) = m^2\sigma^2/2$ . The exact dynamics of the inflaton field are not important, as long as it has a flat enough potential that will generate a period of inflation.

While the inflaton takes care of inflation, the curvaton will generate the curvature perturbations. For simplicity, we will ignore the curvature perturbations generated by the inflaton as described in section 2.3 and the curvature perturbations will be solely due to  $\delta\sigma$ .

The power spectrum obtained for  $\delta\sigma$  will be nearly scale-invariant as before, but after inflation ends, the curvaton will start to oscillate around the minimum of its potential, generating perturbations in the energy density and therefore the curvature.

#### 3.1.1 Curvaton field perturbation

Looking at (3.1), we see that the curvaton, with the same quadratic potential as we used before for the inflaton, essentially has the same Lagrangian and thus obeys the same field equation (2.6). Just like we did with the inflaton, we assume  $\sigma$  is nearly homogenous and in analogy with (2.1) we write:

$$\sigma(\mathbf{x}, t) = \sigma(t) + \delta\sigma(\mathbf{x}, t), \quad (3.2)$$

which leads us to the same equation of motion for the perturbation as before, (2.18):

$$\delta\ddot{\sigma}_{\mathbf{k}} + 3H\delta\dot{\sigma}_{\mathbf{k}} - \left(\frac{k}{a}\right)^2\delta\sigma_{\mathbf{k}} + \frac{1}{2}V''\delta\sigma_{\mathbf{k}} = 0. \quad (3.3)$$

Using the quadratic potential from (3.1), this leads to:

$$\delta\ddot{\sigma} + 3H\delta\dot{\sigma} - \left[ \left( \frac{k}{a} \right)^2 - m^2 \right] \delta\sigma = 0, \quad (3.4)$$

where we dropped the subscript, since we will always be working with the Fourier modes. During inflation, we assume the curvaton is very light  $m^2 \ll H^2$ . Combined with an initial Gaussian perturbation, this will then lead to the same scale invariant spectrum we had before:

$$\mathcal{P}_\sigma = \left( \frac{H}{2\pi} \right)^2 \Big|_{k=aH}. \quad (3.5)$$

### 3.1.2 An evolving curvature perturbation

So far, the curvaton model brings us nothing new. The difference arises when we consider how curvature perturbations are obtained from this field perturbation. In the single field model, the curvature perturbation arising from  $\delta\phi$ , as described in (2.32) freezes out almost instantly after the field perturbation has frozen out, which is just after horizon exit. In general, even for non-Einstein gravity, it has been calculated [20] that the time evolution of the curvature perturbation is given by:

$$\dot{\zeta} = -\frac{H}{\rho + P} \delta P_{\text{nad}} + \text{gradient terms}, \quad (3.6)$$

where  $\delta P_{\text{nad}}$  is the non-adiabatic pressure and we ignore gradient terms because we are working within the separate universe approximation. This means that curvature perturbations will be constant if the pressure perturbation is adiabatic. In the case of the single-field model, this is the case and curvature perturbations freeze out as soon as  $\delta\phi$  does. For the curvaton model, this is not the case.

## 3.2 Curvature perturbations in the curvaton model

In this section we describe how the curvaton field perturbation gives rise to curvature perturbations. We will see that the resulting curvature power spectrum allows for a greater non-Gaussianity than in the single field model.

### 3.2.1 Oscillatory epoch

During inflation, the energy density of the curvaton is negligible compared to that of the inflaton. As the slow-roll conditions fail, the inflaton starts to oscillate and decays, where we assume that it decays predominantly into radiation. The field perturbation  $\delta\sigma$  is now frozen, but as the Hubble rate starts to drop, oscillations

begin around the time when  $H \sim m$ . In order to calculate the curvature perturbation arising from  $\delta\sigma$ , we first calculate the density perturbation it creates, which we denote as:

$$\delta \equiv \frac{\delta\rho_\sigma}{\langle\rho_\sigma\rangle}, \quad (3.7)$$

where  $\delta\rho_\sigma$  contains the spatial inhomogeneity. Again, using the separate universe approximation, we ignore gradients within a Hubble volume and assume that the oscillation is harmonic in each “universe”, with the energy density given by:

$$\rho_\sigma(\mathbf{x}) = \frac{1}{2}m^2\sigma^2(\mathbf{x}), \quad (3.8)$$

with  $\sigma(\mathbf{x})$  the amplitude of oscillation.

Expanding to first order, we can write:

$$\rho_\sigma(\mathbf{x}) = \rho_\sigma + \delta\rho_\sigma = \frac{1}{2}m^2(\sigma + \delta\sigma)^2, \quad (3.9)$$

where  $\rho_\sigma$  and  $\sigma$  are the zeroth order, homogeneous values.

We can now identify two limits. If the field value  $\sigma$  is nonzero and the field slightly fluctuates around this value from region to region in space, we are in the limit  $\delta\sigma \ll \sigma$ . This means that, to zeroth order  $\langle\rho_\sigma\rangle = m^2\sigma^2/2$  and to first order  $\delta\rho_\sigma = m^2\sigma\delta\sigma$ , yielding:

$$\delta = 2\frac{\delta\sigma}{\sigma}. \quad (3.10)$$

However, if  $\sigma$  is very close to zero and the perturbation is big enough, it is possible to be in the regime where  $\delta\sigma \gg \sigma$ , which means the roles  $\sigma$  and  $\delta\sigma$  have in perturbation theory are reversed. To zeroth order we now have  $\langle\rho_\sigma\rangle = m^2\langle(\delta\sigma)^2\rangle/2$ , while to first order  $\delta\rho_\sigma = m^2(\delta\sigma)^2/2$ , which leads to:

$$\delta = \frac{(\delta\sigma)^2}{\langle(\delta\sigma)^2\rangle}. \quad (3.11)$$

Since  $\delta\sigma$  is a Gaussian perturbation, the density perturbation is also Gaussian in the limit  $\delta\sigma \ll \sigma$ , whereas in the opposite limit the density perturbation becomes the square of a Gaussian quantity (a  $\chi^2$  quantity).

### 3.2.2 The curvature perturbation

Now that we have found expressions for the density perturbation, we need to know how this translates into a curvature perturbation. According to (3.6), the curvature perturbation will evolve as long as there is non-adiabatic pressure, which is the case when the energy density of the universe is a mixture of matter and radiation.



This happens when the curvaton starts to oscillate and becomes massive, after which its energy density drops more slowly ( $\propto a^{-3}$ ) than that of radiation ( $\propto a^{-4}$ ) and we enter an epoch of neither matter nor radiation domination. This period with a non-adiabatic pressure perturbation is then sustained until the universe is dominated by a single fluid again. This will be at the time of matter (curvaton) domination, unless the curvaton decays into ultra-relativistic particles before it starts to dominate the energy density. For simplicity we will assume the curvaton decay happens instantaneously when  $H = \Gamma$ .

In analogy with (2.32), the curvature perturbation can be expressed in terms of the density contrast as [20]:

$$\zeta = -H \frac{\delta\rho}{\dot{\rho}}. \quad (3.12)$$

With the energy density proportional to the scale factor  $\rho = a^{-n}\rho_0$ , we have:

$$\dot{\rho} = -na^{-n-1}\dot{a}\rho_0 = -nH\rho, \quad (3.13)$$

where  $n = 3$  for matter and  $n = 4$  for radiation. Since they are both perfect, non-interacting fluids, their energy densities are separately conserved. Plugging this into (3.12) we can calculate the curvature perturbations for both the curvaton and radiation components:

$$\begin{aligned} \zeta_\gamma &= \frac{1}{4} \frac{\delta\rho_\gamma}{\rho_\gamma} \\ \zeta_\sigma &= \frac{1}{3} \frac{\delta\rho_\sigma}{\rho_\sigma} = \frac{\delta}{3}, \end{aligned} \quad (3.14)$$

which can be combined to obtain the total curvature perturbation:

$$\zeta = -H \frac{\delta\rho_\gamma + \delta\rho_\sigma}{\dot{\rho}_\gamma + \dot{\rho}_\sigma} = \frac{4\rho_\gamma\zeta_\gamma + 3\rho_\sigma\zeta_\sigma}{4\rho_\gamma + 3\rho_\sigma}. \quad (3.15)$$

$\zeta_\gamma$  is the curvature perturbation due to the inflaton which has decayed into radiation. However, as we stated before, we ignore curvature perturbations generated in this way, which leads to the simplification:

$$\zeta = \frac{3\rho_\sigma\zeta_\sigma}{4\rho_\gamma + 3\rho_\sigma} = \frac{\rho_\sigma}{4\rho_\gamma + 3\rho_\sigma} \delta, \quad (3.16)$$

from which we can see that the curvature perturbation is a multiple of  $\delta$ . Thus, if  $\delta$  is Gaussian, so is  $\zeta$ . Since this remains valid until after curvaton decay, we can use (3.16) to look at the two different limits discussed earlier.

If the curvaton dominates the energy density before it decays ( $\rho_\sigma \gg \rho_\gamma$ , the curvature perturbation is given by:

$$\zeta = \frac{\delta}{3}. \quad (3.17)$$

If the curvaton decays earlier, when it only contributes a small fraction  $r \ll 1$  to the energy density ( $\rho_\sigma = r\rho_\gamma$ ), the curvature perturbation is:

$$\zeta = \frac{r\delta}{4}. \quad (3.18)$$

Using our earlier results for the density and field perturbation, we can now calculate the curvature power spectrum. In the Gaussian regime (ignoring the factors of  $\frac{1}{3}$  and  $\frac{1}{4}$ ), we have:

$$\mathcal{P}_\zeta = \left( \frac{rH}{\pi\sigma} \right)^2 \Big|_{k=aH} \quad (3.19)$$

where we used the results from (3.5) and (3.10). We could also look in the opposite limit  $\delta\sigma \gg \sigma$ , but this leads to a completely non-Gaussian curvature perturbation, which is excluded by experiment [21]. However, we can look at the intermediate regime where we have a small non-Gaussian component. Combining (3.10) and (3.11) and assuming radiation domination, the curvature perturbation is given by:

$$\zeta = \frac{r}{4} \left[ 2\frac{\delta\sigma}{\sigma} + \left( \frac{\delta\sigma}{\sigma} \right)^2 \right], \quad (3.20)$$

with:

$$\frac{\delta\sigma}{\sigma} = \frac{H}{2\pi\sigma} \Big|_{k=aH}. \quad (3.21)$$

### 3.2.3 Evaluating the non-Gaussianity

As we stated before, the field perturbation (3.21) is Gaussian. However, as we see in (3.20), the curvature perturbation depends not only linearly, but also quadratically on  $\delta\sigma/\sigma$ , which gives a non-Gaussian component to the curvature perturbation. It is important to stress the difference with the single field model. As we described in section 2.3.4, it is also possible to obtain a small amount of non-Gaussianity in the single field model, by including higher orders of  $\delta\phi$  in the Taylor approximation used in (2.32). The crucial difference however, is that in the single field model  $\delta\phi \ll \phi$  always. The curvature perturbation is generated during inflation, when  $\phi$  is still slowly rolling down the potential and has a nonzero mean value. Once the inflaton starts to oscillate and decay, the curvature perturbation is already frozen. Therefore the quadratic term in the Taylor expansion is negligible.

Because the curvaton is subdominant during inflation,  $\sigma \ll \phi$  and  $\delta\sigma/\sigma$  need not be extremely small, which makes the second term in (3.20) non-negligible, leading to a non-Gaussian curvature perturbation. This is the canonical way of generating non-Gaussianities in a curvaton model. However, this thesis focusses on a different way to obtain non-Gaussian curvature perturbations, through a process of *parametric resonant decay*, which will be described in section 4.

### 3.3 The decay channel

In this section we briefly discuss the decay channel for the curvaton.

In section 3.2.2 we assumed the curvaton to decay into radiation instantly at a time when  $H = \Gamma$ . Of course, this is a simple approximation. In reality we assume there is a perturbative decay process which leads to an exponential decay of the curvaton. The decay could proceed through a Yukawa coupling to some light, ultra-relativistic fermion  $\psi$ , by including a Yukawa term to the Lagrangian (3.1):

$$\mathcal{L}_{\text{Yukawa}} = h\sigma\bar{\psi}\psi. \quad (3.22)$$

This adds a second damping factor  $\Gamma\dot{\sigma}$  to the curvaton field equation, leading to a decay rate [4]:

$$\Gamma = \frac{h^2 m}{8\pi}. \quad (3.23)$$

Since the coupling constant  $h$  is basically a free parameter, this means  $\Gamma$  is also free. There is a lower bound on the decay rate though, for if the curvaton decayed very late it would interfere with hot big bang nucleosynthesis, which we assume takes places after all the curvature perturbations are fixed. This leads to a lower bound for the decay rate [22]:

$$\Gamma \gtrsim \frac{T_{\text{BBN}}^2}{m_P}. \quad (3.24)$$

Apart from this lower bound the decay rate is a free parameter. Going back to our previous approximation that the decay would happen instantly at  $H = \Gamma$ , we see that because of the freedom we have in choosing  $\Gamma$ , we were justified to explore both cases where the curvaton decays *before* matter domination (for large  $\Gamma$ ) as well as *after* matter domination (small  $\Gamma$ ).

Another possibility we will not explore here but which is still worth mentioning is curvaton as a candidate for dark matter. In principle the decay process could be such that not all of the curvaton decayed, for instance if there is just a resonant decay and no perturbative decay channel. The curvaton particles left after the resonance would then exist as dark matter.

## 4 Resonant curvaton decay

In this section we will describe the process of resonant curvaton decay (or pre-heating). We describe how a curvaton which is coupled to another field can decay quickly through a parametric resonance. First, we will consider the case in which this other field is also a scalar field  $\chi$ . Then we will discuss the new case in which the curvaton is coupled to a gauge field.

## 4.1 Parametric decay into scalar field

First, we will look at the case where the curvaton is coupled to another scalar field  $\chi$  and decays through a parametric resonance. We modify the standard curvaton Lagrangian (3.1). It now includes canonical kinetic terms  $-\partial^\mu\psi_i\partial_\mu\psi_i/2$  for all scalar fields  $\psi_i$  and it now has a potential:

$$V(\phi, \sigma, \chi) = V(\phi) + \frac{1}{2}m^2\sigma^2 + \frac{1}{2}g^2\sigma^2\chi^2, \quad (4.1)$$

where  $V(\phi)$  is a slow-roll inflaton potential,  $m$  is the curvaton mass and  $g < 1$  a coupling constant. If we want the rest of the curvaton particles, which are left after the resonance, to decay we can include a Yukawa term (3.22).

During inflation, both  $\sigma$  and  $\chi$  are subdominant and at the time of freeze-out  $H_\star$ , we have  $\rho_\sigma, \rho_\chi \ll \rho_\phi = H_\star^2 m_P^2$ . From (4.1) we see that  $\chi$  has an effective mass  $m_{\chi\text{eff}} = g\sigma \gtrsim H_\star$ , where the inequality implies that  $\chi$  is massive during inflation and therefore does not obtain any field perturbations in the same way the curvaton does. If it were light like  $\sigma$ , we would effectively have two curvatons. In order for  $\chi$  to comply with these two conditions: being both subdominant in the energy density and massive during inflation, its value is driven to zero exponentially fast. This also means the  $\chi - \sigma$  interaction term in (4.1) hardly contributes to the effective mass of the curvaton, i.e.  $m^2 \gg g^2\chi^2$ .

After inflation has ended a parametric resonance takes place, in a process similar to that of inflationary preheating [4, 5, 6, 7]. In original preheating, the inflaton particles are annihilated to create  $\chi$  particles. Since at this stage, the inflaton is the dominant energy density, the process of preheating occurs during a period of matter domination. In contrast, in the case of curvaton preheating the dominant contribution of the energy density (inflaton) has already decayed into radiation, so the resonance occurs during a period of radiation domination, which slightly modifies the results of the original inflaton preheating.

### 4.1.1 Evolution of the curvaton

After inflation, the field equation for the curvaton is, in analogy with (2.6):

$$\ddot{\sigma} + 3H\dot{\sigma} + m^2\sigma = 0, \quad (4.2)$$

where we used  $m^2 \gg g^2\chi^2$ . In the case of matter domination  $H = 2/3t$ , whereas during radiation domination  $H = 1/2t$ . We assume the matter component remains subdominant until after the curvaton decay, so we use the latter solution for  $H$ . Now we multiply by  $t^2$  to obtain the standard form of the well known Bessel

equation. The solution to (4.2) is then given by:

$$\begin{aligned}\sigma(t) &= C_1 \frac{J_{1/4}(mt)}{t^{1/4}} && \text{(radiation domination)} \\ \sigma(t) &= C_2 \frac{J_{1/2}(mt)}{t^{1/2}} && \text{(matter domination),}\end{aligned}\tag{4.3}$$

where  $C_1, C_2$  are integration constants. Sticking with the radiation dominated case, we can find the appropriate constant by matching (4.3) with the initial condition  $\sigma(0) = \sigma_*$ . Doing so, the solution becomes:

$$\sigma(t) = 2^{1/4} \Gamma(5/4) \sigma_* \frac{J_{1/4}(mt)}{(mt)^{1/4}}.\tag{4.4}$$

For  $mt < 1$ , the leading term in the Taylor expansion of the Bessel function is cancelled by the factor  $(mt)^{-1/4}$  and  $\sigma$  is nearly constant at  $\sigma_*$ , the value it obtained during inflation. However, when  $H \sim m$ , oscillations begin and as soon as  $mt \gtrsim 1$ , (4.4) can be approximated as a slowly damped oscillator:

$$\sigma(t) \approx \bar{\sigma} \sin\left(mt + \frac{\pi}{8}\right),\tag{4.5}$$

with the decaying amplitude  $\bar{\sigma}$  given by [9]:

$$\bar{\sigma}(t) = \frac{2^{3/4} \Gamma(5/4)}{\pi^{1/2}} \frac{\sigma_*}{(mt)^{3/4}}.\tag{4.6}$$

For simplicity, we assume the oscillations start at  $t_{\text{osc}} = 3\pi/8$  and this also the time where we normalise the scale factor, so henceforth  $a_{\text{osc}} = a(t_{\text{osc}}) = 1$ . After this normalisation, the energy density of the curvaton can be expressed in terms of the density at  $t_{\text{osc}}$ :

$$\rho_\sigma = \frac{m^2 \sigma_{\text{osc}}^2}{2a^3} \equiv \frac{\rho_{\sigma, \text{osc}}}{a^3},\tag{4.7}$$

with

$$\sigma_{\text{osc}} = \frac{8\Gamma(5/4)}{3^{3/4} \pi^{5/4}} \sigma_* \approx 0.76 \sigma_*\tag{4.8}$$

being the value of the curvaton at the time when oscillations start.

The exact solution (4.5) is needed, because the resulting time-dependent frequency in the equation of motion for  $\chi$  leads to the resonance.

#### 4.1.2 The $\chi$ field equation and resonance in a non-expanding universe

Since  $\chi$  is a scalar field, its equation of motion is derived in the same way as we did for the inflaton in section 2.2.1 and is given by (2.16). Using the potential (4.1), this becomes:

$$\ddot{\chi} + 3H\dot{\chi} - (\nabla^2 - g^2\sigma^2)\chi = 0.\tag{4.9}$$

Again, we rather work with the Fourier transform, where the evolution of the modes is given by:

$$\ddot{\chi}_{\mathbf{k}} + 3H\dot{\chi}_{\mathbf{k}} + \left(\frac{k^2}{a^2} + g^2\sigma^2\right)\chi_{\mathbf{k}} = 0, \quad (4.10)$$

which is the equation for a damped oscillator with a time-dependent frequency due to  $a(t)$  and  $\sigma(t)$ .

In the case of a non-expanding universe and small oscillations of  $\sigma$  around a nonzero value  $\sigma_0$ , this can be solved by the theory of the Mathieu equation. Equation (4.10) can then be written in the canonical form of the Mathieu equation

$$\chi_{\mathbf{k}}'' + (\Sigma_{\mathbf{k}} - 2q \cos 2z)\chi_{\mathbf{k}} = 0, \quad (4.11)$$

by shifting variables to  $z = mt + 5\pi/8$ . In (4.11), the prime denotes differentiation with respect to  $z$  and:

$$\Sigma_{\mathbf{k}} = 4 \left( \frac{k^2 + g^2\sigma_0^2}{m^2} \right) \quad q = \frac{4g^2\sigma_0\bar{\sigma}}{m^2}, \quad (4.12)$$

from which we see that the time-dependence of  $q$  must be small in order for the theory of the Mathieu equation to be valid. In the regime of small oscillations around  $\sigma_0$ , where  $\bar{\sigma} \ll \sigma_0 \ll m/g$ , there is such a small time dependence and there are narrow resonance bands,  $q \ll 1$ . In that case there exist exponentially growing solutions  $\chi_{\mathbf{k}} \propto \exp(\mu_{\mathbf{k}}^{(j)} z)$  in the resonance bands labelled by  $j$ . These lead to an exponentially growing particle density for those modes of  $\chi$ :

$$n_{\mathbf{k}}(t) \propto \exp(2\mu_{\mathbf{k}}^{(j)} z). \quad (4.13)$$

### 4.1.3 Stochastic resonance in an expanding universe

In the toy-model case of the non-expanding universe, we have  $q \ll 1$ . However, in order for the resonance to take place in an expanding universe, we require the condition  $q^2 m \gtrsim H$ . By using (4.12) this would mean that

$$\bar{\sigma} g \gtrsim 2m \left( \frac{H}{m} \right)^{1/4}. \quad (4.14)$$

If we ignore the weak  $H^{1/4}$  time dependence and since roughly  $H \sim m$ , this means that for preheating to occur we require  $\bar{\sigma} \gtrsim m/g$ , which is exactly opposite to the condition for resonance in a non-expanding universe. Furthermore, if we assume large fluctuations around the average value for the curvaton field, i.e.  $\bar{\sigma} \gg \sigma_0$ , which is especially true if we assume  $\sigma_0 \approx 0$ , then we have a slightly different Mathieu equation, where the  $q$ -parameter is given by:

$$q = \frac{g^2\bar{\sigma}^2}{4m^2}. \quad (4.15)$$

From the condition on  $\bar{\sigma}$  mentioned above, this means a resonance will only take place for large  $q$  and will end when  $q \lesssim 1/4$ . In fact, in order to get an efficient resonance in an expanding universe we need an initial value  $q_0 \gtrsim 10^3$  at the end of inflation.

In discussing the new  $q$ -parameter (4.15) we have skipped over an important difference with the non-expanding case though. In an expanding universe the Hubble drag term in (4.10) is nonzero thus it is slightly harder to rewrite this equation in the form of a Mathieu equation, (4.11). However, this is possible by rescaling the field as  $X_{\mathbf{k}}(t) = a^{3/2}(t)\chi_{\mathbf{k}}(t)$ . Doing so, we can absorb the Hubble drag term from (4.10) into the second order derivative term and rewrite the equation of motion as:

$$\ddot{X}_{\mathbf{k}} + \omega_{\mathbf{k}}^2 X_{\mathbf{k}} = 0, \quad (4.16)$$

in which the time-dependent frequency  $\omega_{\mathbf{k}}$  is given by:

$$\omega_{\mathbf{k}}^2 = \frac{k^2}{a^2} + g^2 \bar{\sigma}^2 \sin^2 \left( mt + \frac{\pi}{8} \right) - \frac{3\ddot{a}}{2a} - \frac{3}{4} \left( \frac{\dot{a}}{a} \right)^2. \quad (4.17)$$

Here, the last terms are to compensate for the additional terms generated by  $\ddot{X}_{\mathbf{k}}$ . However these terms can be neglected, since

$$\frac{\ddot{a}}{a} \sim \left( \frac{\dot{a}}{a} \right)^2 = H^2 \lesssim m^2 \ll g^2 \bar{\sigma}^2, \quad (4.18)$$

which makes them insignificant compared to the second term. Because of the implicit time dependence of the frequency, due to  $a(t)$  and  $\sigma(t)$ , there is no simple solution to (4.16). However, as an initial condition we can take a positive frequency solution  $X_{\mathbf{k}}(t) \simeq \exp(-i\omega_{\mathbf{k}}t)/\sqrt{2\omega_{\mathbf{k}}}$ . We can write down an adiabatic invariant which can be interpreted as a comoving particle density:

$$n_{\mathbf{k}} = \frac{\omega_{\mathbf{k}}}{2} \left( \frac{|\dot{X}_{\mathbf{k}}|^2}{\omega_{\mathbf{k}}^2} + |X_{\mathbf{k}}|^2 \right) - \frac{1}{2}. \quad (4.19)$$

Although this is the quantity we are interested in, the hard part is to estimate  $X_{\mathbf{k}}$  and its derivative.

As shown in [4], the creation of  $\chi$  particles is most efficient when  $\sigma$  becomes very small, which happens every half-period of curvaton oscillation. However, while the frequency of  $\sigma$  is fixed ( $\omega_{\sigma} = m$ ), the average frequency for  $X$  is decreasing in time due to  $\bar{\sigma} \propto t^{-3/4}$ . At first,  $g\bar{\sigma} \gg m$ , the frequency of  $X$  is much higher and  $X$  oscillates many times as  $\sigma$  changes slightly. However, with time the amplitude of the curvaton oscillation drops, which causes  $X$  to oscillate more slowly. In [4] an example case is taken where  $g = 0.1$  and  $m \sim 10^{-6}m_P$ . Using these parameters it

is calculated that, because of the decreasing field amplitude, the modes  $X_{\mathbf{k}}$  do not stay in one resonance band during an oscillation but actually go through  $\sim 10^3$  resonance bands. In [4] this calculation is performed in the matter dominated case where  $\bar{\sigma} \propto t^{-1}$  and the effect will be less in the radiation dominated case of curvaton preheating, yet the principle remains the same: during a single oscillation,  $X$  will go through many resonance bands. This causes the standard methods for the Mathieu equation in a single resonance band to fail.

In the broad resonance regime where  $q \gg 1$ , there can only be a resonance at “creation moments” where  $\sigma(t) = 0$ . Due to the time dependence of  $a(t)$ , but mostly due to the time dependence of  $\bar{\sigma}(t)$ , the frequency of  $X$  changes dramatically with each oscillation of  $\sigma$ . This causes the phases of  $X_{\mathbf{k}}$  during each oscillation to be uncorrelated, whereas in the case of a non-expanding universe, the phase of  $\chi_{\mathbf{k}}$  is the same at every “creation moment”. Since the particle number (4.19) depends on this phase, the number of particles created at any “creation moment” becomes a stochastic quantity and might in some cases even be negative (such that the resonance destroys particles). However, a broad resonance is still possible since simulations show that in 75% of the cases,  $X_{\mathbf{k}}$  and thus particle number grows during a creation moment. This regime of resonance is called *stochastic resonance*. Stochastic resonance takes part during the early stages of the resonance, when  $q$  is very large. With time,  $q$  decreases and  $\chi$  stays longer in each resonance band. After  $\sim q_0^{1/4}/\sqrt{2\pi}$  oscillations the standard methods for the Mathieu equation apply again and “normal” resonance takes over, which lasts until  $q \lesssim 1/4$  when  $\chi$  settles down into a constant value.

#### 4.1.4 Adiabatic representation and particle density

We can write the solutions to the field equation (4.16) formally as solutions in the adiabatic approximation:

$$X_{\mathbf{k}}(t) = \frac{\alpha_{\mathbf{k}}(t)}{\sqrt{2\omega}} e^{-i \int^t \omega dt} + \frac{\beta_{\mathbf{k}}(t)}{\sqrt{2\omega}} e^{i \int^t \omega dt}, \quad (4.20)$$

where we are interested in the amplitude of the growing modes, which give us the number density  $n_{\mathbf{k}} = |\beta_{\mathbf{k}}|^2$ . In the broad resonance regime, there is only significant particle creation at the creation moments  $t_j$  when  $\sigma(t_j) = 0$ . Everywhere else the field evolves according to (4.20) and the particle number remains constant. The amplitudes  $\alpha_{\mathbf{k}}$  and  $\beta_{\mathbf{k}}$  are constant in this adiabatic regime, but they change significantly between creation moments, so that we can write for  $t_{j-1} < t < t_j$ :

$$X_{\mathbf{k}}^j(t) = \frac{\alpha_{\mathbf{k}}^j}{\sqrt{2\omega}} e^{-i \int^t \omega dt} + \frac{\beta_{\mathbf{k}}^j}{\sqrt{2\omega}} e^{i \int^t \omega dt}. \quad (4.21)$$



This can be interpreted as waves scattering in a parabolic potential, where at every creation moment  $t_j$  there is a reflection and transmission amplitude.

To study the non-adiabatic regime where  $\sigma \approx 0$ , we can Taylor expand the curvaton around  $t = t_j$ :

$$\ddot{X}_{\mathbf{k}} + \left( \frac{k^2}{a^2} + g^2 \bar{\sigma}^2 m^2 (t - t_j)^2 \right) X_{\mathbf{k}} = 0, \quad (4.22)$$

where as before we neglected the terms  $\sim H^2$  in the frequency.

This equation can be brought into a simpler form by changing variables:

$$\frac{d^2 X_{\mathbf{k}}}{d\tau^2} + (\kappa_j^2 + \tau_j^2) X_{\mathbf{k}} = 0, \quad (4.23)$$

with  $\tau_j = k_{\star}(t - t_j)$  and  $\kappa_j = k/ak_{\star}$ , where  $k_{\star} = \sqrt{gm\sigma_{\text{osc}}}$  and  $a$  is to be evaluated at  $t_j$ . The solutions to (4.23) are linear combinations of the parabolic cylinder functions  $W(-\kappa_j/2; \pm\sqrt{2}\tau_j)$ . From these solutions reflection and transmission amplitudes can be extracted, which give a recursion relation between  $(\alpha_{\mathbf{k}}^{j+1}, \beta_{\mathbf{k}}^{j+1})$  and  $(\alpha_{\mathbf{k}}^j, \beta_{\mathbf{k}}^j)$ . These relations can then be used to obtain a recursion relation for the particle density between creation moments. In the limit of large occupation numbers,  $n_{\mathbf{k}} \gg 1$ , this is given by:

$$n_{\mathbf{k}}^{j+1} = n_{\mathbf{k}}^j \exp(2\pi\mu_{\mathbf{k}}^j), \quad (4.24)$$

where

$$\mu_{\mathbf{k}}^j = \frac{1}{2\pi} \ln \left( 1 + 2e^{-\pi\kappa_j^2} - 2 \sin \theta_j e^{-\frac{\pi}{2}\kappa_j^2} \sqrt{1 + e^{-\pi\kappa_j^2}} \right) \quad (4.25)$$

and  $\theta_j$  is an essentially random phase that leads to the stochastic nature of the particle creation. Both terms in (4.25) are proportional to  $e^{-\kappa_j^2} \propto e^{-1/g}$ . This function is non-analytical at  $g = 0$ , which highlights the non-perturbative nature of the resonance. The second term in (4.25) is always positive, so it always leads to particle creation, but the last term can be positive or negative depending on the phase  $\theta_j$ . This leads to very different values for  $\mu^j$ . Although on average  $\sin \theta_j = 0$ , this value can of course vary between  $-1$  and  $1$ , depending on the phase. In the simulations performed in [4] this leads to an average value  $\mu^j \approx 0.18$ , but variations from a maximum of  $\sim 0.28$  to negative values. In the latter case, this means there is actually a drop in particle number during a ‘‘creation moment’’, although on average the particle number will increase.

To obtain the total particle density we must do two things to (4.24): sum over  $j$  and integrate over  $k$ . After a few oscillations of the curvaton, the sum over  $j$  can be approximated by a time integral and:

$$n_{\mathbf{k}}(t) = \frac{1}{2} e^{2\pi \sum_j \mu_{\mathbf{k}}^j} \approx \frac{1}{2} \exp \left( 2m \int^t dt \mu_{\mathbf{k}}(t) \right). \quad (4.26)$$

Furthermore, we can replace the time integral by an effective growth index  $\int^t dt \mu_{\mathbf{k}}(t) = \mu_{\mathbf{k}}^{\text{eff}} t$ . Then we integrate over  $k$  to get the full particle density for  $\chi$ :

$$n_{\chi}(t) = \frac{1}{(2\pi a)^3} \int d^3 k n_{\mathbf{k}}(t) = \frac{1}{4\pi^2 a^3} \int dk k^2 \exp(2m\mu_{\mathbf{k}}^{\text{eff}} t). \quad (4.27)$$

Because of the exponential dependence on  $\mu_{\mathbf{k}}^{\text{eff}}$ , which has a maximum value  $\mu \equiv \max(\mu_{\mathbf{k}}^{\text{eff}})$  at  $k = k_{\text{max}}$ , (4.27) can be solved by the method of steepest descent:

$$n_{\chi}(t) \simeq \frac{1}{8\pi^2 a^3} \frac{\Delta k k_{\text{max}}^2 e^{2\mu t}}{\sqrt{\pi \mu t}}, \quad (4.28)$$

where  $\Delta k$  is the width of the resonance band and typically  $k_{\text{max}} \sim \Delta k \sim k_{\star}/2$ , which implies:

$$n_{\chi}(t) \approx \frac{k_{\star}^3}{64\pi^2 a^3 \sqrt{\pi \mu t}} e^{2\mu t}. \quad (4.29)$$

#### 4.1.5 Back-reaction

As the number density of  $\chi$  particles grows exponentially, we get to a stage where there are so many  $\chi$  particles that back-reaction effects of  $\chi$  particles decaying into curvatons can no longer be ignored. When this happens, our linear approach fails and we need a full nonlinear treatment of the resonance, which can be done using lattice methods [9]. This back-reaction stage is obtained when the contribution of  $\chi$  to the effective curvaton mass becomes roughly equal to the bare mass, so when  $g^2 \langle \chi^2 \rangle \sim m^2$ . Since number density is given by:

$$n_{\chi} \sim \frac{\rho_{\chi}}{m_{\chi}^{\text{eff}}} \approx \frac{g^2 \sigma^2 \langle \chi^2 \rangle}{g\sigma} = \langle \chi^2 \rangle g\sigma, \quad (4.30)$$

we can find the back-reaction time by equating this with  $m^2\sigma/g$  and plugging it in (4.29) as the particle density. Squaring both sides and taking the logarithm, we obtain:

$$t_{\text{br}} \approx \frac{1}{4m\mu} \ln \left( \frac{10^5 \mu m (m t_{\text{br}})^{5/2}}{g^5 \sigma_{\text{osc}}} \right), \quad (4.31)$$

where we used  $\sigma(t_{\text{br}}) = \sigma_{\text{osc}} \approx 0.76\sigma_{\star}$  and  $a = (8mt/3\pi)^{1/2}$ . The solution to (4.31) is given by the lower branch of the Lambert W function:

$$t_{\text{br}} \approx -\frac{5}{8m\mu} W_{-1} \left( -10^{-2} g^{8/5} / m u^{3/5} q_{\text{osc}}^{1/5} \right). \quad (4.32)$$

## 4.2 The curvature perturbation

In the previous section we discussed the parametric resonance and obtained an expression for the back-reaction time, beyond which our linear approach fails. So if we want to study the curvature perturbations created by the resonance, the best we can do is to study the perturbation at this time. However, if we assume the resonance ends instantly at  $t_{\text{br}}$ , we don't have to deal with the nonlinear regime. In the following we assume that after  $t_{\text{br}}$  the perturbative curvaton decay, as discussed in section 3.3, takes over.

### 4.2.1 Separate universe approximation revisited

In order to calculate the curvature perturbation generated by the resonance, we have to go back to the separate universe approximation as introduced in section 2.3.1. From (2.31) we see that in order to find the curvature perturbation, we need the scale factor at the time of back-reaction. Since the scale factor depends on the energy density, we would like to write down the relation between the two at the time of back-reaction. However, after the resonance the fields go through a period of nonlinear, non-equilibrium dynamics, which makes calculations (near) impossible. Instead, we will calculate the scale factor and energy density by comparing them to their values at some reference time  $t_{\text{ref}}$  well after the resonance has ended:

$$\rho = \rho_{\text{ref}} \left[ r_{\text{ref}} \left( \frac{a_{\text{ref}}}{a} \right)^3 + (1 - r_{\text{ref}}) \left( \frac{a_{\text{ref}}}{a} \right)^4 \right], \quad (4.33)$$

with  $r_{\text{ref}}$  the matter fraction of the energy density at  $t_{\text{ref}}$ . We assume  $\chi$  to be ultra-relativistic, so the only contribution to the matter energy density will come from the curvaton. Although we assume that  $r_{\text{ref}} \ll 1$ , not all of the curvaton particles decay during the resonance and the remaining ones will decay later through a perturbative decay process as described in section 3.3. To find an expression for  $\ln a$ , we invert (4.33), giving:

$$a^4 = a_{\text{ref}}^4 \frac{\rho_{\text{ref}}}{\rho} \left[ r_{\text{ref}} \left( \frac{a}{a_{\text{ref}}} \right) + (1 - r_{\text{ref}}) \right]. \quad (4.34)$$

Since we assume radiation domination, to good approximation  $\rho \propto a^{-4}$ , so we can make the replacement  $(a/a_{\text{ref}}) = (\rho_{\text{ref}}/\rho)^{1/4}$ . Doing so and taking the logarithm on both sides gives:

$$4 \ln a = 4 \ln a_{\text{ref}} + \ln \frac{\rho_{\text{ref}}}{\rho} + \ln \left[ 1 + r_{\text{ref}} \left( \left( \frac{\rho_{\text{ref}}}{\rho} \right)^{1/4} - 1 \right) \right]. \quad (4.35)$$

With the matter fraction being so small,  $\epsilon \equiv r_{\text{ref}} \left( \left( \frac{\rho_{\text{ref}}}{\rho} \right)^{1/4} - 1 \right) \ll 1$ , we can Taylor expand  $\ln(1 + \epsilon)$ . Doing so gives us the final expression for  $\ln a$ :

$$\ln a = \ln a_{\text{ref}} + \frac{1}{4} \left[ \ln \frac{\rho_{\text{ref}}}{\rho} + r_{\text{ref}} \left( \left( \frac{\rho_{\text{ref}}}{\rho} \right)^{1/4} - 1 \right) \right]. \quad (4.36)$$

From (2.31) we see that to obtain the curvature perturbation, we need to differentiate (4.36) with respect to the curvaton field value during inflation. The first two terms are given by [9]:

$$(\ln a)'|_{\rho} = (\ln a_{\text{ref}})' + \frac{1}{4} \left[ \left( 1 + \frac{r}{4} \right) \frac{\rho'_{\text{ref}}}{\rho_{\text{ref}}} + (r - r_{\text{ref}}) \frac{r'_{\text{ref}}}{r_{\text{ref}}} \right] \quad (4.37)$$

$$\begin{aligned} (\ln a)''|_{\rho} = (\ln a_{\text{ref}})'' + \frac{1}{4} \left[ \frac{\rho''_{\text{ref}}}{\rho_{\text{ref}}} - \left( \frac{\rho'_{\text{ref}}}{\rho_{\text{ref}}} \right)^2 + \frac{r}{4} \left( \frac{\rho''_{\text{ref}}}{\rho_{\text{ref}}} - \frac{3}{4} \left( \frac{\rho'_{\text{ref}}}{\rho_{\text{ref}}} \right)^2 \right) \right. \\ \left. + \frac{r}{2} \frac{r'_{\text{ref}}}{r_{\text{ref}}} \frac{\rho'_{\text{ref}}}{\rho_{\text{ref}}} + (r - r_{\text{ref}}) \frac{r''_{\text{ref}}}{r_{\text{ref}}} \right]. \end{aligned} \quad (4.38)$$

These results can be applied to any curvaton model, with or without a parametric resonance. In the models without a resonance, as studied in section 3, the curvature perturbation can be calculated at the time of perturbative decay, which in section 3.3 we assumed to happen instantaneously at  $H = \Gamma$ .

## 4.2.2 Curvature perturbation without resonance

We would like to test the validity of equations (4.37) by applying them first to the case where there is no resonance. In this case, we have already calculated the curvature perturbation in section 3.2.2 and we can see whether we get the same results using the expressions (4.37).

As a reference time we can use the time at which oscillations start ( $t_{\text{ref}} = t_{\text{osc}}$ ), because without a resonance, the energy density evolves like (4.33) at all times. Since oscillations start when  $H \sim m$  we get, by the Friedmann equation,  $\rho_{\text{ref}} = \rho_{\text{osc}} = m^2 m_P^2$  and this expression does not depend on  $\sigma_*$ . Since the scale factor depends hardly on the matter energy density,  $a_{\text{ref}}$  too is independent of  $\sigma_*$ . So the only relevant derivative is  $r'$ . This massively simplifies (4.37):

$$\begin{aligned} (\ln a)'|_{\rho} &= \frac{1}{4} (r - r_{\text{osc}}) \frac{r'_{\text{osc}}}{r_{\text{osc}}} \\ (\ln a)''|_{\rho} &= \frac{1}{4} (r - r_{\text{osc}}) \frac{r''_{\text{osc}}}{r_{\text{osc}}}. \end{aligned} \quad (4.39)$$

With  $r_{\text{osc}} = \rho_{\sigma, \text{osc}} / \rho_{\text{osc}} = m^2 \sigma_{\text{osc}}^2 / 2\rho_{\text{osc}}$ , the two derivatives can easily be calculated. As we did in section 3.2.2, we evaluate the curvature perturbation just before the (instantaneous) perturbative decay, hence we assume  $r_{\text{osc}} \ll r \ll 1$ . Doing so yields the curvature perturbation up to second order:

$$\zeta = \frac{r}{4} \left[ 2 \frac{\delta\sigma_\star}{\sigma_\star} + 2 \left( \frac{\delta\sigma_\star}{\sigma_\star} \right)^2 \right]. \quad (4.40)$$

Comparing this with (3.20), we can see the equations aren't quite the same. This is because in (3.20) we combined the first order expansion of two different limits. If we stayed in the limit  $\delta\sigma \ll \sigma$  and expanded (3.18) to second order:

$$\zeta = \frac{r}{4} (\delta + \delta^2/2). \quad (4.41)$$

the resulting curvature perturbation would be the same as (4.40).

We can also use the results (4.39) to calculate the nonlinearity parameter  $f_{\text{NL}}$  of the curvature perturbation. Plugging (4.39) into (2.44) gives:

$$f_{\text{NL}} = \frac{5}{6} \frac{(\ln a)''}{(\ln a)'^2} \Big|_\rho = \frac{20}{6} \frac{r_{\text{osc}}}{r - r_{\text{osc}}} \frac{r_{\text{osc}}''}{r_{\text{osc}}'^2} \quad (4.42)$$

and by using  $r_{\text{osc}} = m^2 \sigma_{\text{osc}}^2 / 2\rho_{\text{osc}}$  and the fact that  $r_{\text{osc}} \ll r$ , this reduces to:

$$f_{\text{NL}} = \frac{5}{3r}, \quad (4.43)$$

where  $r$  is the matter fraction at the time of the perturbative decay.

### 4.2.3 Curvature perturbation from resonant decay

The previous section was just a recap of the curvature perturbation generated without a resonance. Our real interest lies in calculating the curvature perturbation generated by the resonant decay as discussed in section 4.1. This was done by [9].

Since the linear approach used in section 4.1 breaks down past the point of back-reaction, we assume the resonance ends abruptly at  $t_{\text{br}}$  and use this as our reference time. So combining the back-reaction time (4.32) with our normalisation for the scale factor  $a = (t/t_{\text{osc}})^{1/2}$ , we can calculate the scale factor at this time. Then we can use equations (4.38) to give [9]:

$$\begin{aligned} (\ln a_{\text{br}})' &\approx -\frac{1}{2} (\ln \mu)' - \frac{1}{3\pi\mu a_{\text{br}}^2 \sigma_\star} (1 + \mathcal{O}(a_{\text{br}}^2)) \\ (\ln a_{\text{br}})'' &\approx -\frac{1}{2} (\ln \mu)'' + \frac{1}{3\pi\mu a_{\text{br}}^2 \sigma_\star} (1 + \mathcal{O}(a_{\text{br}}^2)). \end{aligned} \quad (4.44)$$

These expressions involve derivatives of  $\mu$  and it is hard to estimate how this parameter will depend on the curvaton freeze-out value, which is why we will just leave this expression as it is.

We want to calculate the curvature perturbation at some time after the resonance. If the resonance ends at  $t_{\text{br}}$ , a fraction  $\xi$  of the curvaton energy density is transferred into ultra-relativistic  $\chi$ -particles, so just after back-reaction the energy densities for matter and radiation are given by:

$$\begin{aligned}\rho_{\sigma,br} &= (1 - \xi) \frac{\rho_{\sigma,osc}}{a_{\text{br}}^3} \\ \rho_{\gamma,br} &= \frac{\rho_{\gamma,osc}}{a_{\text{br}}^4} + \xi \frac{\rho_{\sigma,osc}}{a_{\text{br}}^3},\end{aligned}\quad (4.45)$$

from which we can calculate the total energy density and matter fraction at back-reaction:

$$\begin{aligned}\rho_{\text{br}} &= \frac{\rho_{\sigma,osc}}{a_{\text{br}}^3} + \frac{\rho_{\gamma,osc}}{a_{\text{br}}^4} \approx \frac{\rho_{\text{osc}}}{a_{\text{br}}^4} (1 + r_{\text{osc}}(a_{\text{br}} - 1)) \\ r_{\text{br}} &= \frac{\rho_{\sigma,br}}{\rho_{\text{br}}} \approx \frac{\rho_{\sigma,br}}{\rho_{\gamma,br}} \approx (1 - \xi) r_{\text{osc}} a_{\text{br}}.\end{aligned}\quad (4.46)$$

Plugging these and the leading order terms from (4.44) into (4.37) yields:

$$\begin{aligned}(\ln a)'|_{\rho} &= \frac{r}{4} \left[ \frac{\xi}{1 - \xi} \frac{a_{\text{br}}}{a} \left( \frac{2}{\sigma_{\star}} - \frac{1}{2} \frac{\mu'}{\mu} + \frac{\xi'}{\xi} \right) + \frac{2}{\sigma_{\star}} - \frac{\xi'}{1 - \xi} \right] \\ (\ln a)''|_{\rho} &= \frac{r}{4} \left[ \frac{\xi}{1 - \xi} \frac{a_{\text{br}}}{a} \left( \frac{2}{\sigma_{\star}^2} + \frac{4}{\sigma_{\star}} \left( \frac{\xi'}{\xi} - \frac{1}{2} \frac{\mu'}{\mu} \right) + \frac{\xi''}{\xi} + \frac{(\mu^{-1/2})''}{\mu^{-1/2}} - \frac{\xi' \mu'}{\xi \mu} \right) \right. \\ &\quad \left. + \frac{2}{\sigma_{\star}^2} - \frac{4\xi'}{\sigma_{\star}(1 - \xi)} - \frac{\xi''}{1 - \xi} \right].\end{aligned}\quad (4.47)$$

The terms scaling as  $a^{-1}$  in the above equations represent radiation inhomogeneities due to the resonant decay. Since the curvature perturbation stops evolving once all the curvaton particles have decayed, these  $a^{-1}$  terms will be irrelevant if the perturbative lifetime  $1/\Gamma$  of the curvaton is large. In that case we ignore those terms, which hugely simplifies (4.47):

$$\begin{aligned}(\ln a)' &\sim \frac{r}{2\sigma_{\star}} \left( 1 - \frac{\sigma_{\star}^2 \xi'}{2(1 - \xi)} \right) \\ (\ln a)'' &\sim \frac{r}{2\sigma_{\star}^2} \left( 1 - \frac{2\sigma_{\star} \xi'}{1 - \xi} - \frac{\sigma_{\star}^2 \xi''}{2(1 - \xi)} \right),\end{aligned}\quad (4.48)$$

which gives the curvature perturbation:

$$\zeta = \frac{r}{2} \left[ \frac{\delta\sigma_{\star}}{\sigma_{\star}} \left( 1 - \frac{\sigma_{\star}^2 \xi'}{2(1 - \xi)} \right) + \frac{\delta\sigma_{\star}^2}{\sigma_{\star}^2} \left( 1 - \frac{2\sigma_{\star} \xi'}{1 - \xi} - \frac{\sigma_{\star}^2 \xi''}{2(1 - \xi)} \right) \right].\quad (4.49)$$

If we set  $\xi = 0$ , which corresponds to the case without a resonance, we can see that (4.49) reduces to (4.40).

Just like we did in the previous section, we can also calculate the non-linearity parameter in the case of the resonant decay. Again, we plug (4.48) into (2.44) to give:

$$f_{\text{NL}} = \frac{5}{3r} \left( 1 - \frac{2\sigma_*\xi'}{1-\xi} - \frac{\sigma_*^2\xi''}{2(1-\xi)} \right) \left( 1 - \frac{\sigma_*\xi'}{2(1-\xi)} \right)^{-2}, \quad (4.50)$$

in the limit where the terms  $\propto a^{-1}$  in (4.37) have redshifted away.

### 4.3 Gauge coupled curvaton resonance

In section 4.1 we discussed how the curvaton could decay into another scalar field through a parametric resonance. We will now consider the same process for a curvaton which is charged under a U(1) gauge group. The gauge field is in its vacuum state during inflation, but as the curvaton starts to oscillate, a resonance can occur which creates excitations in the gauge field (photons). Although preheating into a U(1) gauge field has been studied briefly in [23], a different coupling between the scalar and gauge-field is used there.

In our case, the Lagrangian is that of ordinary scalar electrodynamics, although the inner products are altered by the fact we are working in curved spacetime. It is given by

$$\mathcal{L} = \mathcal{L}_\phi - \frac{1}{4}F_{\mu\nu}F^{\mu\nu} - \frac{1}{2}D_\mu\sigma^*D^\mu\sigma - V(\sigma^*\sigma), \quad (4.51)$$

where  $D^\mu\sigma = (\partial^\mu + ieA^\mu)\sigma$ . Since this is quite a different Lagrangian to what we had before in (4.1), we must not only derive the field equation for  $A_\mu$ , but also re-derive the curvaton field equation. For simplicity, we choose to work in the Weyl gauge where  $A_0 = 0$ .

#### 4.3.1 Evolution of the curvaton

To derive the equation of motion for the curvaton, we go back to (2.13), which for complex fields becomes:

$$\begin{aligned} \square\sigma - \frac{\partial V(\sigma^*\sigma)}{\partial\sigma^*} &= 0 \\ \square\sigma^* - \frac{\partial V(\sigma^*\sigma)}{\partial\sigma} &= 0. \end{aligned} \quad (4.52)$$

However, the d'Alembertian is now somewhat more complicated, since we have to replace  $\partial_\mu$  with  $D_\mu$ , the gauge covariant derivative. Using (2.15) and making the

replacement  $\partial_\mu \rightarrow D_\mu$ , the d'Alembertian term can be rewritten as:

$$\square\sigma = \frac{1}{\sqrt{-g}}D_\mu(\sqrt{-g}g^{\mu\nu}D_\nu\sigma), \quad (4.53)$$

with  $\sqrt{-g} = a^3$ . Ignoring gradients in  $\sigma$  as we did before and using the Weyl gauge  $A_0 = 0$ , (4.53) can be rewritten as:

$$\square\sigma = -\ddot{\sigma} - 3H\dot{\sigma} + iea^{-2}\partial_i A_i\sigma - e^2a^{-2}A^2\sigma, \quad (4.54)$$

where  $A^2 = \mathbf{A} \cdot \mathbf{A}$ . Combining this with (4.52) and using a quadratic potential for the curvaton,  $V(\sigma^*\sigma) = m^2|\sigma|^2$ , we obtain the equation of motion for the curvaton:

$$\ddot{\sigma} + H\dot{\sigma} + \left(\frac{e^2A^2 - ie\partial_i A_i}{a^2} + m^2\right)\sigma = 0 \quad (4.55)$$

and in the same way:

$$\ddot{\sigma}^* + H\dot{\sigma}^* + \left(\frac{e^2A^2 + ie\partial_i A_i}{a^2} + m^2\right)\sigma^* = 0. \quad (4.56)$$

Since  $A_\mu$  is in the vacuum state during inflation, we assume it hardly contributes to the effective mass of the curvaton, i.e.  $e^2A^2/a^2 \ll m^2$ , until so many photons are created that the two terms become equal in strength and we can no longer ignore the back-reaction. For the same reason we also ignore the gradient term and the field equations for  $\sigma$  and  $\sigma^*$  become equal to (4.2). Therefore, we can treat the curvaton in exactly the same way as we did in section 4.1.1, which means the solution for  $\sigma$  (and its complex conjugate) is still approximately given by (4.5).

### 4.3.2 The gauge field equation

To derive the gauge field equation of motion, we start from the Lagrangian (4.51) and use the Euler-Lagrange equations, which have to be modified slightly since we are working in curved spacetime. The volume element in the action  $d^4x \rightarrow \sqrt{-g}d^4x$ , which means we can still use the Euler-Lagrange equations if we replace  $\mathcal{L} \rightarrow \sqrt{-g}\mathcal{L}$ :

$$\partial_\nu \left( \frac{\partial(\sqrt{-g}\mathcal{L})}{\partial(\partial_\nu A_\mu)} \right) - \frac{\partial(\sqrt{-g}\mathcal{L})}{\partial A_\mu} = 0. \quad (4.57)$$

Using the Lagrangian (4.51), this becomes:

$$\partial_\nu(\sqrt{-g}F^{\mu\nu}) + \frac{ie\sqrt{-g}}{2}(\sigma\partial^\mu\sigma^* - \sigma^*\partial^\mu\sigma) + \sqrt{-g}e^2|\sigma|^2A^\mu = 0, \quad (4.58)$$



where  $F^{\mu\nu} = g^{\mu\alpha}g^{\nu\beta}F_{\alpha\beta}$ . We use this to work out the first term, where we note that the metric does not depend on any spatial coordinates. After some math, we obtain:

$$\partial_\nu(\sqrt{-g}F^{\mu\nu}) = a^3(-3Hg^{\mu\alpha}F_{\alpha 0} - g\mu\alpha_{,0}F_{\alpha 0} + g^{\mu\alpha}g^{\nu\beta}F_{\alpha\beta,\nu}). \quad (4.59)$$

Then we use the fact that the metric is diagonal, while diagonal entries of the asymmetric field tensor are zero to simplify this expression. Doing so and plugging it back into (4.58) yields:

$$a^3 [g^{\mu j}(-3HF_{j0} - F_{j0,0} + a^{-2}F_{j,i,i}) - g_{,0}^{\mu j}F_{j0} + g^{\mu 0}a^{-2}F_{0i,i}] + \frac{iea^3}{2}(\sigma\partial^\mu\sigma^* - \sigma^*\partial^\mu\sigma) + a^3e^2|\sigma|^2A^\mu = 0, \quad (4.60)$$

which can be split into two different equations. The dynamical equation is the one where  $\mu = j$ , which gives the equation of motion for the field  $\mathbf{A}$ . The  $\mu = 0$  equation would give the equation of motion for  $A_0$ , but since we are in Weyl gauge this equation actually becomes a constraint equation (Gauss's law) on  $\mathbf{A}$ .

Let us first consider this constraint equation by setting  $\mu = 0$  in (4.60). Since the metric is diagonal and we work in Weyl gauge, most terms drop out and we are left with:

$$a\partial_0(\partial_i A_i) + a^3\frac{ie}{2}(\sigma^*\dot{\sigma} - \dot{\sigma}^*\sigma) = 0. \quad (4.61)$$

Since  $E_i = -\partial_0 A_i$  this is essentially Gauss' law:

$$\nabla \cdot \mathbf{E} = \rho, \quad (4.62)$$

with the charge density given by  $\rho = (ie/2a^2)(\sigma^*\dot{\sigma} - \dot{\sigma}^*\sigma)$ .

Next we consider the more interesting dynamical equation of motion. Setting  $\mu = j$  in (4.60) and lowering the index on  $A^j$  gives:

$$aHF_{j0} + aF_{j0,0} - a^{-1}F_{j,i,i} - ae^2|\sigma|^2A_j = 0, \quad (4.63)$$

where as before we ignored gradients in the curvaton. After dividing by a, expanding the field tensors and using the Weyl gauge ( $A_0 = 0$ ), we obtain the field equation for the spatial vector field  $\mathbf{A}$ :

$$\ddot{\mathbf{A}} + H\dot{\mathbf{A}} + \nabla(\nabla \cdot \mathbf{A}) - \nabla^2\mathbf{A} + e^2|\sigma|^2\mathbf{A} = 0, \quad (4.64)$$

where as before  $\nabla_j = a^{-1}\partial_j$ . We can Fourier transform (4.64) to obtain the equation of motion for the modes of  $\mathbf{A}$ . We separately consider the longitudinal and transverse modes of  $\mathbf{A}$ . For the (unphysical) longitudinal modes, the third

and fourth term cancel each other, while for the transverse modes, the divergence term drops out. In the end, the equations of motion become:

$$\ddot{A}_{\mathbf{k}}^L + H\dot{A}_{\mathbf{k}}^L + e^2|\sigma|^2 A_{\mathbf{k}}^L = 0 \quad (\text{longitudinal modes})(4.65)$$

$$\ddot{A}_{\mathbf{k}}^T + H\dot{A}_{\mathbf{k}}^T + \left(\frac{k^2}{a^2} + e^2|\sigma|^2\right) A_{\mathbf{k}}^T = 0 \quad (\text{transverse modes}). (4.66)$$

In order to solve these equations, we rescale the fields like we did in section 4.1.3. By rescaling  $B_{\mathbf{k}} = a^{1/2}A_{\mathbf{k}}$ , we can absorb the Hubble drag term into the two other terms. The resulting equation of motion becomes:

$$\ddot{B}_{\mathbf{k}} + \omega_{\mathbf{k}}^2 B_{\mathbf{k}} = 0, \quad (4.67)$$

with the frequency for the transverse modes given by:

$$\omega_{\mathbf{k}}^2 = \frac{k^2}{a^2} + e^2|\sigma|^2 - \frac{1}{2}\frac{\ddot{a}}{a} + \frac{1}{4}\left(\frac{\dot{a}}{a}\right)^2 \quad (4.68)$$

As before we ignore the last two terms  $\sim H^2$ . Then (4.67) can be written in the form of a Mathieu equation (4.11) with:

$$\Sigma_{\mathbf{k}} = \frac{k^2}{a^2 m^2} + \frac{e^2 \bar{\sigma}^2}{2m^2} \quad \text{and} \quad q = \frac{e^2 \bar{\sigma}^2}{4m^2}. \quad (4.69)$$

This is almost exactly identical to the evolution of the  $\chi$  modes discussed in section 4.1. As we discussed in that section, the resonance only takes place for  $q^2 m \gtrsim H$ , which means  $q \gtrsim 1/4$ . And since  $q$  decays very rapidly ( $\propto (mt)^{-3/2}$ ) this requires a large initial value for  $q$ . Therefore, after a few oscillations, modes  $A_{\mathbf{k}}$  go through many resonance bands in a single oscillation and we are required to once again use the framework of stochastic resonance as developed in [4].

### 4.3.3 Stochastic resonance of the gauge field

Since the evolution of the transverse modes of  $\mathbf{A}$  is dictated by the same equation of motion as that of the scalar modes  $X_{\mathbf{k}}$ , cf. (4.67) and (4.16), we use the same framework to study the resonance. In analogy with (4.19) the number density per comoving volume for photons created during the resonance is given by:

$$n_{\mathbf{k}} = \frac{\omega_{\mathbf{k}}}{2} \left( \frac{|\dot{B}_{\mathbf{k}}|^2}{\omega_{\mathbf{k}}^2} + |B_{\mathbf{k}}|^2 \right) - \frac{1}{2}, \quad (4.70)$$

for each of the two transverse polarisations. Just like before we can write the formal solution to (4.67) as an adiabatic expansion:

$$B_{\mathbf{k}}(t) = \frac{\alpha_{\mathbf{k}}(t)}{\sqrt{2\omega}} e^{-i \int^t \omega dt} + \frac{\beta_{\mathbf{k}}(t)}{\sqrt{2\omega}} e^{i \int^t \omega dt}. \quad (4.71)$$

Now, just like before, we assume the coefficients to be constant in between creation moments  $t_j$  where  $\sigma(t_j) = 0$ . In between those moments, which occur every half-period of the curvaton oscillation, the modes  $B_{\mathbf{k}}$  evolve adiabatically according to (4.71) which leads to the exact analogy of (4.21):

$$B_{\mathbf{k}}^j(t) = \frac{\alpha_{\mathbf{k}}^j}{\sqrt{2\omega}} e^{-i \int^t \omega dt} + \frac{\beta_{\mathbf{k}}^j}{\sqrt{2\omega}} e^{i \int^t \omega dt}, \quad (4.72)$$

which is valid for  $t_{j-1} < t < t_j$ . Further steps are also the same as in the scalar case: to study the non-adiabatic regime we Taylor expand  $|\sigma|^2$  at times  $t_j$  like in (4.22). The solution to this gives us parabolic cylinder functions which yield recursion relations for  $\alpha_j$  and  $\beta_j$ . Using the relation  $n_{\mathbf{k}} = |\beta_{\mathbf{k}}|^2$ , these can then be used to obtain a recursion relation for the number density of created photons (4.24). Just like before, we can approximate the sum over  $j$  by an integral and the photon density for each of the two transverse polarisations will be given by (4.26):

$$n_{\mathbf{k}}(t) = \frac{1}{2} \exp(2m\mu_{\mathbf{k}}^{\text{eff}}t), \quad (4.73)$$

where we already made the replacement  $\int_0^t \mu_{\mathbf{k}}(t) dt \rightarrow \mu_{\mathbf{k}}^{\text{eff}}t$ .

Although number density is not an entirely well-defined quantity for photons, we assume that for the modes of the electromagnetic field the following relation holds:

$$\rho_{\mathbf{k}}(t) = \omega_{\mathbf{k}} n_{\mathbf{k}} = \frac{\omega_{\mathbf{k}}}{2} \exp(2m\mu_{\mathbf{k}}^{\text{eff}}t) \quad (4.74)$$

for each transverse polarisation. A further ambiguity arises when we want to identify this frequency. Do we just use  $\omega_{\mathbf{k}} = k/a$ , or do we identify it with the full frequency (4.68)? (excluding the terms  $\sim H^2$ ) We will discuss this in the next section and for the moment implicitly write  $\omega_{\mathbf{k}}$ .

#### 4.3.4 Back-reaction

Just like in the case of the scalar field resonance, we would like to figure out the back-reaction time  $t_{\text{br}}$  at which the back-reaction of the gauge field can no longer be ignored. This is the case when the contribution of  $\mathbf{A}$  to the effective mass of the curvaton becomes similar to the bare mass, or  $e^2 \langle \mathbf{A} \cdot \mathbf{A} \rangle \sim m^2$ . So, just like in the scalar case, we need to find the expectation value of the field squared. However, whereas in the scalar case there was an easy relation between the field value squared and the energy density (4.30), this is not the case for the gauge field.

From basic electromagnetism we know that the energy stored in an electromagnetic field configuration is given by:

$$\rho = \frac{1}{2}(E^2 + B^2), \quad (4.75)$$

with  $E$  and  $B$  the magnitudes of the electric and magnetic fields, respectively. In the absence of electric charge  $\mathbf{E} = -\partial_0\mathbf{A}$  and  $\mathbf{B} = \nabla \times \mathbf{A}$ , so after Fourier transforming this we can see that the electromagnetic energy in each mode is given by:

$$\rho_{\mathbf{k}}(t) = \frac{1}{2}(|\dot{\mathbf{A}}_{\mathbf{k}}|^2 + 2k^2(A_{\mathbf{k}}^T)^2), \quad (4.76)$$

where in the second term we have replaced the cross product by the nonzero transverse components and the factor 2 comes from the fact there are two transverse directions. Given the energy density, this expression gives us the sum of the field value squared and its derivative, which is not what we want to know. We cannot subtract the  $\dot{\mathbf{A}}$  term though, because we are using this formula to find the gauge field value in the first place. Therefore we make the assumption that we can use the virial theorem, which states that the kinetic and potential energy contributions are roughly equal. Although this has been proven only for systems in thermal equilibrium, in many cases it holds long before a system has reached equilibrium. We can view the  $\dot{\mathbf{A}}$  term as a kinetic energy, with  $(A^T)^2$  being the potential energy term. Using the virial theorem they are of roughly the same size, which gives us as an approximation:

$$\rho_{\mathbf{k}}(t) \approx 2k^2(A_{\mathbf{k}}^T)^2. \quad (4.77)$$

By applying the techniques from [4] we have obtained the energy density in (4.74) and we need to obtain  $\langle \mathbf{A}(-\mathbf{k}) \cdot \mathbf{A}(\mathbf{k}) \rangle = \langle (A_{\mathbf{k}}^L)^2 + 2(A_{\mathbf{k}}^T)^2 \rangle$ . Since (4.77) only gives us a relation between the energy density and the transverse modes, we need to look further into the size and physical meaning of the longitudinal modes. These modes evolve according to (4.65) and are subject to the Gauss constraint (4.61). Focussing on (4.65), we can see that the longitudinal modes evolve according to a Mathieu equation, but that there is no gradient term. If we rescale these modes and bring the equation of motion in the form (4.67), we see that for the longitudinal modes the frequency does not depend on  $k$ . This means the modes do not obey a wave equation and therefore do not propagate through space. Instead, these modes correspond to a field oscillating independently at each point in space with a frequency  $\omega^2 = e^2|\sigma|^2$ , if we again ignore terms  $\sim H^2$  in (4.68).

The longitudinal modes also behave like a Mathieu equation, but because there is no  $k$ -dependence of the frequency, we cannot apply the methods from [4] as used in section 4.1.4. In particular, we cannot approximate the equation of motion for the longitudinal modes by an equation of the form (4.23). Because of their unphysical nature we ignore the contribution of the longitudinal modes to  $\langle \mathbf{A} \cdot \mathbf{A} \rangle$ . The real term in the Lagrangian is  $\langle A_\mu A^\mu \rangle$  anyway, where we already ignored the  $A_0$  contribution. So we replace  $\langle A_\mu A^\mu \rangle \rightarrow \langle \mathbf{A} \cdot \mathbf{A} \rangle \rightarrow \langle (A^T)^2 \rangle$ . Under this assumption and combining this with (4.77) yields:

$$\langle \mathbf{A}(-\mathbf{k}) \cdot \mathbf{A}(\mathbf{k}) \rangle = \left\langle \frac{\rho_{\mathbf{k}}}{k^2} \right\rangle. \quad (4.78)$$

Next, we plug in twice the value for  $\rho_{\mathbf{k}}$  from (4.74) (because this expression was for each of the two transverse polarisations) and integrate over all  $k$  to give:

$$\langle \mathbf{A} \cdot \mathbf{A} \rangle = \int \frac{d^3k}{(2\pi a)^3} \frac{\omega_{\mathbf{k}}}{k^2} \exp(2m\mu_{\mathbf{k}}^{\text{eff}}t). \quad (4.79)$$

As we stated before, we now need to determine which frequency to use in this equation. We will first do the calculation using  $\omega_{\mathbf{k}} = k/a$  and afterwards we will include the  $e^2|\sigma|^2$  term from (4.68).

Let us first consider the simple case where  $\omega_{\mathbf{k}} = k/a$ . Plugging this into (4.79) the integral becomes:

$$\langle \mathbf{A} \cdot \mathbf{A} \rangle = \frac{1}{2\pi^2 a^4} \int dk k \exp(2m\mu_{\mathbf{k}}^{\text{eff}}t). \quad (4.80)$$

Just like in the case of the scalar field resonance, the growth index  $\mu_{\mathbf{k}}^{\text{eff}}$  has a maximum at  $k_m$ , with value  $\mu \equiv \mu_{k_m}^{\text{eff}}$ , which can be used to calculate the integral in (4.80) by the method of steepest descent:

$$\langle \mathbf{A} \cdot \mathbf{A} \rangle \simeq \frac{1}{4\pi^2 a^4} \frac{k_m e^{2\mu t} \Delta k}{\sqrt{\pi \mu m t}}. \quad (4.81)$$

As in section 4.1.4 we pick  $k_m \sim \Delta k \sim k_*/2$  with  $k_* = \sqrt{em\sigma_{\text{osc}}}$  to give

$$\langle \mathbf{A} \cdot \mathbf{A} \rangle \approx \frac{1}{16\pi^2 a^4} \frac{k_m^2}{\sqrt{\pi \mu m t}} e^{2\mu t}. \quad (4.82)$$

As mentioned earlier, we assume the back-reaction of the photons to become important when  $\langle \mathbf{A} \cdot \mathbf{A} \rangle \sim m^2/e^2$ . So equating (4.82) with  $m^2/e^2$  gives:

$$e^{2\mu t_{\text{br}}} = \frac{16\pi^2 m^2 a^4 \sqrt{\pi \mu m t_{\text{br}}}}{k_*^2 e^2}, \quad (4.83)$$

where  $a$  is to be evaluated at  $t_{\text{br}}$ . Using  $a = (8mt/3\pi)^{1/2}$  as before and plugging in  $k_* = \sqrt{em\sigma_{\text{osc}}}$  we get:

$$e^{2\mu t_{\text{br}}} = \left( \frac{2^{10} m^3 t_{\text{br}}^2 \sqrt{\pi \mu m t_{\text{br}}}}{9e^3 \sigma_{\text{osc}}} \right) \quad (4.84)$$

and after squaring both sides and taking the logarithm, this gives us an expression for the back-reaction time:

$$t_{\text{br}} = \frac{1}{4m\mu} \ln \left( \frac{10^5 \mu m^2 (m t_{\text{br}})^5}{e^6 \sigma_{\text{osc}}^2} \right). \quad (4.85)$$

Now, let us repeat this calculation in the case where we take the frequency to be  $\omega_{\mathbf{k}}^2 = k^2/a^2 + e^2|\sigma|^2$ . Because we are looking at the behaviour after many curvaton oscillations and since the amplitude of the curvaton  $\bar{\sigma}$  is quickly decreasing, we approximate the damped oscillator  $\sigma^2$  by its average value over oscillations, which means we substitute  $\sin^2(mt + \pi/8)$  by its average value  $1/2$ , which means that:

$$|\sigma|^2 = \frac{\bar{\sigma}^2}{2} \approx \frac{0.37\sigma_{\text{osc}}^2}{(mt)^{3/2}}, \quad (4.86)$$

where we used (4.6) in the last step. This means the frequency becomes:

$$\omega_{\mathbf{k}} = \left( \frac{k^2}{a^2} + \frac{0.37e^2\sigma_{\text{osc}}^2}{(mt)^{3/2}} \right)^{1/2}. \quad (4.87)$$

Plugging this into (4.79) and using the method of steepest descent in order to calculate the integral, we obtain:

$$\begin{aligned} \langle \mathbf{A} \cdot \mathbf{A} \rangle &= \frac{1}{4\pi^2 a^4} \frac{\Delta k e^{2\mu mt}}{\sqrt{\pi\mu mt}} \left( \frac{k_m^2 (mt)^{3/2} + 0.37e^2\sigma_{\text{osc}}^2}{(mt)^{3/2}} \right)^{1/2} \\ &= \frac{1}{16\pi^2 a^4} \frac{k_* e^{2\mu mt}}{\sqrt{\pi\mu mt}} \left( \frac{k_*^2 (mt)^{3/2} + 0.37e^2\sigma_{\text{osc}}^2}{(mt)^{3/2}} \right)^{1/2}. \end{aligned} \quad (4.88)$$

Just like before, we find the time of back-reaction by equating this with  $m^2/e^2$ . Doing so, using  $a = (8mt/3\pi)^{1/2}$  and squaring both sides,

$$e^{4\mu mt_{\text{br}}} = \left( \frac{10^5 \mu m^3 (mt_{\text{br}})^{13/2}}{e^5 \sigma_{\text{osc}}} \right) \frac{1}{k_*^2 (mt_{\text{br}})^{3/2} + 0.37\sigma_{\text{osc}}^2 e^2 a^2}, \quad (4.89)$$

which reduces to the relation (4.85) in the case where the second term in the denominator is negligible. This is the case when  $t_{\text{br}} \gg 0.1e^2\sigma_{\text{osc}}^2/m^3$ .

We first assume this is the case and use (4.85) as the relation for the back-reaction time, the solution to which is given by the lower branch of the Lambert W-function. In analogy with (4.32) we have:

$$t_{\text{br}} \approx -\frac{5}{4m\mu} W_{-1}(-10^{-1} e^{4/5} \mu^{4/5} q_{\text{osc}}^{1/5}), \quad (4.90)$$

with  $q_{\text{osc}} = e^2\sigma_{\text{osc}}^2/4m^2$ . Under the same assumptions as used in [9] we can then approximate this by:

$$t_{\text{br}} \sim \frac{1}{4m\mu} \ln(10^5 e^{-4} \mu^{-4} q_{\text{osc}}^{-1}), \quad (4.91)$$

which can be used to calculate whether the  $\sigma_{\text{osc}}^2 a^2$  term in the denominator of (4.89) can indeed be neglected. The condition for this was  $t_{\text{br}} \gg 0.1e^2\sigma_{\text{osc}}^2/m^3 =$

$0.4q_{\text{osc}}/m$ . Since large initial values for  $q$  are needed to make sure the resonance takes place at all, we assume  $q \sim 10^3$ . Then, using typical values  $\mu \approx 0.14$  and  $e = 0.1$  we can calculate from (4.91) that:

$$t_{\text{br}} \approx \frac{63}{m} < \frac{0.4q_{\text{osc}}}{m}, \quad (4.92)$$

which means the condition for neglecting the  $\sigma_{\text{osc}}^2 a^2$  term in (4.89) does not hold. Even though the chosen values for  $\mu$  and particularly  $e$  might be way off (the latter could be a few orders of magnitude smaller), this is still a valid conclusion. Those parameters are within the logarithm and changing them by orders of magnitude will only slightly modify the value 63, while  $0.4q_{\text{osc}} \approx 400$ . Clearly, neglecting the  $\sigma_{\text{osc}}^2 a^2$  term in (4.89) is invalid.

Conversely, we can check what happens if we neglect the  $k_\star^2$  term from the denominator of (4.89), which in this case reduces to:

$$e^{4\mu m t_{\text{br}}} = \frac{10^5 \mu m^3 (m t_{\text{br}})^{11/2}}{e^7 \sigma_{\text{osc}}^3}, \quad (4.93)$$

the solution to which is given by:

$$t_{\text{br}} \approx -\frac{11}{8\mu m} W_{-1} \left( -10^{-1} e^{8/11} \mu^{9/11} q_{\text{osc}}^{3/11} \right). \quad (4.94)$$

Under similar assumptions as in (4.91), this is approximately:

$$t_{\text{br}} \sim \frac{1}{8\mu m} \ln \left( 10^{11} e^{-8} \mu^{-9} q_{\text{osc}}^{-3} \right) \quad (4.95)$$

and using the same values as before gives:

$$t_{\text{br}} \approx \frac{61}{m}. \quad (4.96)$$

Because we are now neglecting the other term, the condition on  $t_{\text{br}}$  obviously reverses and is given by  $t_{\text{br}} \ll 0.4q_{\text{osc}}/m \approx 400/m$ . Since 61 is smaller than 400 by about factor 7 this condition is not perfectly satisfied, but it holds to a much better extent than in the case where we only considered the  $k_\star^2$  term in (4.89).

This means that the  $e^2 |\sigma|^2$  term dominates the frequency (4.87) and the back-reaction time is given by (4.94).

#### 4.4 Curvature perturbation from gauge-field resonance

Using the back-reaction time (4.94) we would like to calculate the curvature perturbation using the separate universe approximation as discussed in section 4.2.1.

To do this, we must first calculate the scale factor at the time of back-reaction. Using  $a = (8mt/3\pi)^{1/2}$ , this is given by:

$$a_{\text{br}} \approx \left(-\frac{11}{3\pi\mu}\right)^{1/2} W_{-1}^{1/2}(-10^{-1}e^{8/11}\mu^{9/11}q_{\text{osc}}^{3/11}). \quad (4.97)$$

Then we need to plug this into (4.37) in order to find the terms  $(\ln a)'$  and  $(\ln a)''$  required to calculate the curvature perturbation in the separate universe approximation. In (4.47) we only used the leading order terms from  $(\ln a_{\text{br}})'$  and  $(\ln a_{\text{br}})''$ . In the case of the gauge field resonance, these leading order terms remain the same. Therefore, to leading order, the final expression for the two derivatives of  $\ln a$  are still given by (4.37).

The difference arises, however, in the nature of the parameter  $\xi$ . As before, this denotes the fraction of the curvaton energy density which is converted into radiation. As we can see from (4.37), the curvature perturbation depends heavily on the first and second derivatives of both  $\mu$  and  $\xi$ . The former is the same as before, because in order to calculate the number density of photons created during the resonance, we used the same framework as in the scalar case. The fraction  $\xi$  however, has a different physical origin than in the case of the scalar resonance and therefore its derivatives may be very different, leading to a very different final result for the curvature perturbation.

The same goes for the nonlinearity parameter, which is still given by (4.50) but again might be of very different magnitude than in the scalar case, because of the possible differences in  $\xi'$  and  $\xi''$ .

## 5 Discussion

In this final section, we review our findings for the gauge-coupled resonance and compare them with the scalar resonance. Finally, we look ahead to future numerical work, which could allow for calculating the resonance through the fully nonlinear regime.

### 5.1 Comparison with scalar resonance

In section 4.4 we briefly touched on the differences in the curvature perturbation generated by the scalar resonance and the gauge-coupled resonance. In this section we will look into the similarities and differences between the two cases in more detail.

The methods from original preheating [4] have already been applied to a curvaton model [8]. In this thesis we found that it is also possible to apply these



methods to the case of a gauge-coupled curvaton, as long as we ignore the unphysical longitudinal modes of the gauge field. Furthermore, because the original methods of preheating lead to a number density of created particles, we had to assume a simple relation between the photon number density and energy density. Lastly, by invoking the virial theorem, we assumed the electric and magnetic contributions to the energy density are roughly equal: an assumption which should be subject to further research.

Next, let us compare the actual back-reaction times. In the case of the scalar resonance this is given by (4.32), whereas for the gauge-coupled case it is given by (4.94), which we approximated to be  $61/m$ . Using the same parameters to make an estimate for the back-reaction time in the scalar case,  $\mu = 0.14$  and  $g = 0.1$ , we get  $t_{\text{br}} \approx 48/m$ . This shows that the time of back-reaction is not significantly different between the scalar and gauge-coupled resonances.

One of the important results from section 4.3.4 is that the frequency of the photons  $\omega_{\mathbf{k}}$  on average seems to be dominated by the “interaction term”  $e^2|\sigma|^2$ . We looked at the difference in back-reaction time obtained by using the “bare frequency”  $\omega_{\mathbf{k}} = k/a$  and by using just the “interaction term” and found that the back-reaction times obtained were again nearly identical, cf. (4.92) and (4.96). However, we have shown the latter to be the correct expression, since the interaction term dominates the  $k/a$  term in the denominator of (4.89).

The important difference is that, although the back-reaction times may be fairly similar between the two cases, the dynamics at this time may be very different. As discussed in section 4.4, the final expression for the curvature perturbation is no different for the gauge-coupled resonance as it is in the scalar case. The difference lies with the physical origin of the parameter  $\xi$ , which has a (potentially) different  $\sigma_*$ -dependence. Because this parameter depends on what happens in the nonlinear regime it is important to extend the calculation into this regime, by using numerical simulations.

## 5.2 Numerical simulations

In our calculation of the curvature perturbations from curvaton preheating, we assumed the resonance stopped at  $t_{\text{br}}$ , because our linearised equations broke down at this point. In general, the resonance will continue after back-reaction and to fully calculate the resulting curvature perturbation, one needs to use a full nonlinear simulation.

In [9], lattice field theory methods are used to perform the nonlinear calculations in the case of the scalar resonance. Because the equations of motion in the case of the gauge-coupled resonance are of a similar form to those of the scalar resonance, it is likely that the methods used in [9] will be applicable to the gauge-coupled resonance.

Earlier we discussed how the form of the final curvature perturbation in both scalar and gauge-coupled case were given by the same expression, based on (4.37). Performing a full nonlinear simulation might provide more insight in how the resulting curvature perturbation is varies between the two cases.

## References

- [1] A. H. Guth, *Inflationary Universe: A possible solution to the horizon and flatness problem*, *Phys. Rev. D* **23** (1981) 347-356.
- [2] E. Komatsu *et al.*, *Seven-Year Wilkinson Microwave Anisotropy Probe (WMAP) Observations: Cosmological Interpretation*, *Astrophys. J. Suppl.* **192** (2010) 18.
- [3] J. A. Tauber *et al.*, *Planck pre-launch status: The Planck mission*, *Astronomy & Astrophysics* **520** (2010) A1.
- [4] L. Kofman, A. D. Linde and A. A. Starobinsky, *Towards the theory of reheating after inflation*, *Phys. Rev. D* **56** (1997) 3258-3295.
- [5] L. Kofman, A. D. Linde and A. A. Starobinsky, *Reheating after inflation*, *Phys. Rev. Lett.* **73** (1994) 3195-3198.
- [6] Y. Shtanov, J. H. Traschen and R. H. Brandenberger, *Universe Reheating after Inflation*, *Phys. Rev. D* **51** (1995) 5438-5455.
- [7] J. H. Traschen and R. H. Brandenberger, *Particle production during out-of-equilibrium phase transitions*, *Phys. Rev. D* **42** (1990) 2491-2504.
- [8] K. Enqvist, S. Nurmi and G. I. Rigopoulos, *Parametric Decay of the Curvaton*, *JCAP* **10** (2008) 013.
- [9] A. Chambers, S. Nurmi and A. Rajantie, *Non-Gaussianity from resonant curvaton decay*, *JCAP* **1001** (2010) 012.
- [10] J. P. Preskill, *Cosmological Production of Superheavy Magnetic Monopoles*, *Phys. Rev. Lett.* **43** (1979) 1365-1368.
- [11] S. W. Hawking, I. G. Moss and J. M. Stewart, *Bubble collisions in the very early universe*, *Phys. Rev. D* **26** (1981) 2681-2693.
- [12] [http://ned.ipac.caltech.edu/level5/Watson/Watson5\\_3.html](http://ned.ipac.caltech.edu/level5/Watson/Watson5_3.html)

- [13] A. D. Linde, *A new inflationary universe scenario: a possible solution of the horizon, flatness, homogeneity, isotropy and monopole problems*, *Phys. Lett. B* **108** (1982) 389-392.
- [14] A. Albrecht and P. J. Steinhardt, *Cosmology for Grand Unified Theories with Radiatively Induced Symmetry Breaking*, *Phys. Rev. Lett.* **48** (1982) 1220-1223.
- [15] H. Georgi and S. L. Glashow, *Unity of All Elementary-Particle Forces*, *Phys. Rev. Lett.* **32** (1974) 438-441.
- [16] A. R. Liddle and D. H. Lyth, *Cosmological Inflation and Large-Scale Structure* (Cambridge University Press, 2000) pp 178.
- [17] D. S. Salopek and J. R. Bond, *Nonlinear evolution of long wavelength metric fluctuations in inflationary models*, *Phys. Rev. D* **62** (1990) 3936-3962.
- [18] A. D. Linde and V. Mukhanov, *Nongaussian Isocurvature Perturbations from Inflation*, *Phys. Rev. D* **56** (1997) 535-539.
- [19] D. H. Lyth and D. Wands *Generating the curvature perturbation without an inflaton*, *Phys. Lett. B* **524** (2002) 5-14.
- [20] D. Wands, K. A. Malik, D. H. Lyth and A. R. Liddle, *A new approach to the evolution of cosmological perturbations on large scales*, *Phys. Rev. D* **62** 04352.7 (2000).
- [21] H. A. Feldman, J. A. Frieman, J. N. Fry and R. Scoccimarro, *Constraints on Galaxy Bias, Matter Density, and Primordial Non-Gaussianity from the PSCz Galaxy Redshift Survey*, *Phys. Rev. Lett.* **86** (2001) 1434.
- [22] D. H. Lyth, *Can the curvaton paradigm accommodate a low inflaton decay*, *Phys. Rev. D* **55** (2004) 239-244.
- [23] C. Armendariz-Picon, M. Trodden and E. J. West *Preheating in Derivatively-Coupled Inflation Models*, *JCAP* **0804** (2008) 036.